

# Majorana neutrinos, neutrino mass spectrum, $CP$ violation, and neutrinoless double $\beta$ decay: The three-neutrino mixing case

S. M. Bilenky

Joint Institute for Nuclear Research, Dubna, Russia  
and Scuola Internazionale Superiore di Studi Avanzati, I-34014 Trieste, Italy

S. Pascoli and S. T. Petcov\*

Scuola Internazionale Superiore di Studi Avanzati, I-34014 Trieste, Italy  
and Istituto Nazionale di Fisica Nucleare, Sezione di Trieste, I-34014 Trieste, Italy  
(Received 20 February 2001; published 10 August 2001)

Assuming three-neutrino mixing and massive Majorana neutrinos, we study the implications of the neutrino oscillation solutions of the solar and atmospheric neutrino problems and of the results of the CHOOZ experiment for the predictions of the effective Majorana mass in neutrinoless double-beta  $[(\beta\beta)_{0\nu}]$  decay,  $|\langle m \rangle|$ . The general case of  $CP$  nonconservation is investigated. The predicted values of  $|\langle m \rangle|$ , which determine the magnitude of the  $(\beta\beta)_{0\nu}$ -decay rate, depend strongly on the type of neutrino mass spectrum and on the solution of the solar neutrino problem, as well as on the values of the two Majorana  $CP$ -violating phases, present in the lepton mixing matrix. We find that (i)  $|\langle m \rangle| \leq 0.02$  eV for a hierarchical neutrino mass spectrum, (ii)  $|\langle m \rangle| \leq 0.09$  eV if the spectrum is of the inverted hierarchy type, and (iii)  $|\langle m \rangle| \leq m$  in the case of three quasidegenerate neutrinos,  $m > 0$  being the common neutrino mass scale which is limited by the bounds from the  ${}^3\text{H}$   $\beta$ -decay experiments,  $m < 2.5$  eV. The indicated maximal values of  $|\langle m \rangle|$  are reached in cases (i), (ii), and (iii), respectively, for the large mixing angle (LMA) MSW solution, the small mixing angle (SMA) MSW solution, and for all current solutions of the solar neutrino problem. If  $CP$  invariance holds,  $|\langle m \rangle|$  is very sensitive to the values of the relative  $CP$  parities of the massive Majorana neutrinos. The cases of neutrino mass spectra which interpolate between the hierarchical or inverted hierarchy type and the quasidegenerate one are also studied. The observation of the  $(\beta\beta)_{0\nu}$  decay with a rate corresponding to  $|\langle m \rangle| \geq 0.02$  eV can provide unique information on the neutrino mass spectrum. Combined with information on the lightest neutrino mass or the type of neutrino mass spectrum, it can give also information on the  $CP$  violation in the lepton sector and, if  $CP$  invariance holds, on the relative  $CP$  parities of the massive Majorana neutrinos.

DOI: 10.1103/PhysRevD.64.053010

PACS number(s): 14.60.Pq, 23.40.-s

## I. INTRODUCTION

The observation of a significant up-down asymmetry in the rate of (multi-GeV)  $\mu$ -like events produced by the atmospheric  $\nu_\mu$  and  $\bar{\nu}_\mu$  in the Super-Kamiokande experiment [1] brought to a new level the investigation of the neutrino mass and neutrino mixing problem: for the first time model-independent experimental evidence for neutrino oscillations was obtained. Important evidence for the existence of neutrino mixing was found in experiments with solar neutrinos as well: in all five experiments Homestake, Kamiokande, SAGE, GALLEX, and Super-Kamiokande, which have provided data on the solar neutrino flux so far [2–7] (see also [8,9]), considerably smaller signals than expected [10] were observed. These results are compatible with a depletion of the solar  $\nu_e$  flux on the way to the Earth, i.e., with the disappearance of the solar  $\nu_e$ . Indications for  $\bar{\nu}_\mu \leftrightarrow \bar{\nu}_e$  oscillations were reported by the accelerator LSND experiment [11].

The existing evidence for nonzero neutrino masses and neutrino mixing will be thoroughly tested in the next genera-

tion of neutrino oscillation experiments. The Super-Kamiokande results on the oscillations of the atmospheric neutrinos will be checked in the accelerator long-base-line experiments K2K [12], MINOS [13], and in the CERN-Gran-Sasso (CNGS) experiment [14]; K2K is taking data while MINOS and CNGS experiments are under preparation. The solar neutrino experiments SNO [9], which began operation approximately a year and a half ago, BOREXINO [15], and the reactor antineutrino experiment KamLAND [16] will provide new crucial information on the oscillations of solar neutrinos. Both BOREXINO and KamLAND detectors are under construction and are expected to be operative in 2002. The Liquid Scintillation Neutrino Detector (LSND) results on  $\bar{\nu}_\mu \leftrightarrow \bar{\nu}_e$  oscillations will be tested in the accelerator experiment MiniBooNE [17] which is under preparation.

The high-intensity neutrino beams from a neutrino factory, with known and well-controlled spectra and fluxes, will allow us to study the neutrino oscillation phenomena in considerable detail [18]. These studies can provide, in particular, very precise information on the values of neutrino-mass-squared differences and of the elements of the neutrino (lepton) mixing matrix. The possibility of building a neutrino factory is extensively being investigated at present [19].

There is no doubt that the indicated experimental studies will allow us to take a big step forward in the understanding

\*Also at the Institute of Nuclear Research and Nuclear Energy, Bulgarian Academy of Sciences, 1784 Sofia, Bulgaria.

of the patterns of neutrino-mass-squared differences and of neutrino mixing. However, no information about the absolute values of the neutrino masses and about the physical nature of the neutrinos with definite mass can be obtained in these experiments.

The problem of the nature of massive neutrinos (see, e.g., [20])—whether they are Dirac particles possessing distinctive antiparticles or Majorana fermions, i.e., truly neutral particles identical with their antiparticles—is one of the fundamental problems in studies of neutrino mixing. In the minimal version of the standard theory the individual lepton charges  $L_e$ ,  $L_\mu$ , and  $L_\tau$  are conserved and neutrinos are massless. Massive Dirac neutrinos and neutrino mixing arise in gauge theories in which the lepton charges  $L_e$ ,  $L_\mu$ , and  $L_\tau$  are not conserved, but a specific combination of the latter, which could be the total lepton charge  $L=L_e+L_\mu+L_\tau$  or, e.g., the charge [21]  $L'=L_e-L_\mu+L_\tau$ , is conserved. Thus, the existence of massive Dirac neutrinos is associated in gauge theories with massive neutrinos with the presence of a conserved lepton charge. Massive Majorana neutrinos arise if no lepton charge is conserved by electroweak interactions. Thus, the question of the nature of massive neutrinos is directly related to the question of the fundamental symmetries of elementary particle interactions.

The relative smallness of the neutrino masses, following from the data, can be naturally explained by violation of the total lepton charge conservation at a scale which is much larger than the electroweak symmetry breaking scale<sup>1</sup> [22]. In this case neutrinos with definite mass are Majorana particles. Thus, establishing the Majorana nature of massive neutrinos could imply the existence of a new fundamental scale in physics.

Experiments studying the oscillations of neutrinos cannot answer the question regarding the nature of massive neutrinos [23,24].<sup>2</sup> Neutrino oscillations, in particular, are not sensitive to the Majorana  $CP$ -violating phases [23,26] which enter into the expression for the lepton mixing matrix in the case of massive Majorana neutrinos and which are absent if the massive neutrinos are Dirac particles. Thus, the neutrino oscillation experiments cannot provide also information on  $CP$  violation caused by the Majorana  $CP$ -violating phases and, in the case of  $CP$  invariance, on the relative  $CP$  parities of the massive Majorana neutrinos.

The Majorana nature of the massive neutrinos can manifest itself in the existence of processes in which the total lepton charge  $L$  is not conserved and changes by two units,  $\Delta L=2$ . The process most sensitive to the existence of mas-

sive Majorana neutrinos (coupled to the electron) is the neutrinoless double  $\beta[(\beta\beta)_{0\nu}]$  decay of certain even-even nuclei (see, e.g., [27,20]):

$$(A,Z)\rightarrow(A,Z+2)+e^-+e^-. \quad (1)$$

If the  $(\beta\beta)_{0\nu}$  decay is generated *only by the left-handed (LH) charged current weak interaction through the exchange of virtual massive Majorana neutrinos*, the probability amplitude of this process is proportional in the case of Majorana neutrinos having masses not exceeding a few MeV to the so-called “effective Majorana mass parameter,”

$$\langle m \rangle \equiv \sum_{j=1} U_{ej}^2 m_j, \quad (2)$$

where  $m_j$  is the mass of the Majorana neutrino  $\nu_j$  and  $U_{ej}$  is the element of neutrino (lepton) mixing matrix.

A large number of experiments are searching for  $(\beta\beta)_{0\nu}$  decay of different nuclei at present (for a rather complete list see, e.g., [28]). No indications that this process takes place were found so far. A rather stringent constraint on the value of the effective Majorana mass parameter was obtained in the <sup>76</sup>Ge Heidelberg-Moscow experiment [29]:

$$|\langle m \rangle| < 0.35 \text{ eV}, \quad 90\% \text{ C.L.} \quad (3)$$

Taking into account a factor of 3 uncertainty associated with the calculation of the relevant nuclear matrix element (see, e.g., [27,28]) we get

$$|\langle m \rangle| < (0.35-1.05) \text{ eV}. \quad (4)$$

The IGEX Collaboration has obtained [30]

$$|\langle m \rangle| < (0.33-1.35) \text{ eV}, \quad 90\% \text{ C.L.} \quad (5)$$

Considerably higher sensitivity to the value of  $|\langle m \rangle|$  is planned to be reached in several  $(\beta\beta)_{0\nu}$ -decay experiments of a new generation. The NEMO3 experiment [31], scheduled to start in 2001, will search for  $(\beta\beta)_{0\nu}$  decay of <sup>100</sup>Mo and <sup>82</sup>Se. In its first stage, after 5 years of data taking, this experiment will reach a sensitivity to values of  $|\langle m \rangle| \cong 0.1 \text{ eV}$ . A similar sensitivity is planned to be reached with the cryogenic detector CUORE [32] which will search for the  $(\beta\beta)_{0\nu}$  decay of <sup>130</sup>Te. An order of magnitude better sensitivity, i.e., to  $|\langle m \rangle| \cong 10^{-2} \text{ eV}$ , is planned to be achieved in the GENIUS experiment [33] utilizing 1 ton of enriched <sup>76</sup>Ge. Finally, there is a very interesting proposal [34] to study the  $(\beta\beta)_{0\nu}$  decay of <sup>136</sup>Xe in a background-free experiment with detection of the two electrons and the <sup>+</sup>Ba atom in the final state. The estimated sensitivity of this experiment is  $|\langle m \rangle| \cong (1-5) \times 10^{-2} \text{ eV}$ .

Having in mind future progress in experimental searches for  $(\beta\beta)_{0\nu}$  decay, we derive in the present article constraints on the effective Majorana mass that can be obtained from analyses of the latest neutrino oscillation data. More specifically, assuming three-neutrino mixing and massive Majorana neutrinos, we study in detail the implications of the neutrino oscillation fits of the solar and atmospheric neutrino data and of the results of the reactor long-base-line CHOOZ and Palo

<sup>1</sup>Let us note that this explanation is by no means unique.

<sup>2</sup>If the massive neutrinos are Majorana particles, e.g., the *transitions*  $\nu_l \rightarrow \bar{\nu}_l$ ,  $l=e,\mu,\tau$  are effectively possible [25]. However, the amplitudes of these transitions are proportional to the ratio  $m_j/E$ ,  $m_j$ , and  $E$  being the neutrino mass and energy. For the values of the neutrino masses suggested by the existing <sup>3</sup>H  $\beta$ -decay data and the data on the oscillations of the solar and atmospheric neutrinos (see Sec. II),  $m_j \lesssim \text{few eV}$ , the transitions  $\nu_l \rightarrow \bar{\nu}_l$  are unobservable at present.

Verde experiments, for the predictions of the effective Majorana mass parameter  $|\langle m \rangle|$ , which controls the  $(\beta\beta)_{0\nu}$ -decay rate. We consider the possible types of the neutrino mass spectrum: hierarchical, with two quasidegenerate in mass Majorana neutrinos (the third having a different mass) and with three quasidegenerate Majorana neutrinos. In the case of two quasidegenerate massive neutrinos, the neutrino mass spectrum can be of three varieties—with inverted hierarchy, with partial hierarchy, and with partial inverted hierarchy—and they are also considered in this paper.

The indicated approach for obtaining the values of  $|\langle m \rangle|$  which are compatible with solar, atmospheric, and accelerator neutrino oscillation data was first used in Refs. [35] and [36]. In Ref. [37] it was noticed that in the case of a neutrino mass spectrum with inverted hierarchy and large mixing angle (LMA) Mikheyev-Smirnov-Wolfenstein (MSW) solution of the solar neutrino problem, measurement of  $|\langle m \rangle|$  can give information about the  $CP$  violation in the lepton sector, induced by the Majorana  $CP$ -violating phases.<sup>3</sup> Various aspects of  $CP$  violation in the lepton sector, generated by the Majorana  $CP$ -violating phases, were studied, e.g., in [38–41]. The approach indicated above was further exploited, e.g., in Refs. [42–45]. In Refs. [46–48], in which the solar and atmospheric neutrino data available in 1998–1999 were used, it was concluded, in particular, that observation of  $(\beta\beta)_{0\nu}$  decay with a rate within the sensitivity of the next generation of  $(\beta\beta)_{0\nu}$ -decay experiments can give information about the neutrino mass spectrum. Further analyses along the indicated lines were performed more recently in [49–53].

In the present study we investigate the general case of  $CP$ -nonconservation and we use the results of the analyses of the latest solar and atmospheric neutrino data. For each of the five types of possible neutrino mass spectra indicated above we give detailed predictions for  $|\langle m \rangle|$  for the three solutions of the solar neutrino problem favored by the current solar neutrino data: the LMA MSW, the small mixing angle (SMA) MSW, the LOW-quasivacuum oscillation (LOW-QVO) one. In each case we identify the “just- $CP$ -violation” region of values of  $|\langle m \rangle|$ : a value of  $|\langle m \rangle|$  in this region would unambiguously signal the existence of  $CP$  violation in the lepton sector, caused by Majorana  $CP$ -violating phases. Analyzing the case of  $CP$  conservation, we derive predictions for  $|\langle m \rangle|$  corresponding to all possible values of the relative  $CP$  parities of the three massive Majorana neutrinos for the five different types of neutrino mass spectra. The possibility of cancellation between the different terms contributing to  $|\langle m \rangle|$  is investigated. We identify the cases when such a cancellation is impossible and there exist nontrivial lower bounds on  $|\langle m \rangle|$  and we give these bounds. We find, in particular, that the observation of  $(\beta\beta)_{0\nu}$  decay with a rate corresponding to  $|\langle m \rangle| \geq 0.02$  eV can provide unique information on the neutrino mass spec-

trum. Combined with data on the mass of the lightest neutrino and/or on the type of neutrino mass spectrum, it can give also information on the  $CP$  violation in the lepton sector and, if  $CP$  invariance holds, on the relative  $CP$  parities of the massive Majorana neutrinos.

In the present article we consider only the mixing of the three-flavor neutrinos, involving three massive Majorana neutrinos. We assume that  $(\beta\beta)_{0\nu}$  decay is induced by the  $(V-A)$  charged current weak interaction via the exchange of the massive Majorana neutrinos. Results for the case of four-neutrino mixing will be presented in a separate publication [54].

## II. NEUTRINO MASSES AND MIXING FROM THE EXISTING DATA

We summarize in the present section the data on the neutrino masses, neutrino-mass-squared differences, and neutrino (lepton) mixing which will be used in our further analyses.

Strong evidence for neutrino oscillations has been obtained in experiments with atmospheric and solar neutrinos. The Super-Kamiokande atmospheric neutrino data [1,55] are best interpreted in terms of (dominant)  $\nu_\mu \rightarrow \nu_\tau$  and  $\bar{\nu}_\mu \rightarrow \bar{\nu}_\tau$  oscillations [55]. Assuming two-neutrino mixing, one obtains a description of the data at 90% (99%) C.L. for the following values of the relevant two-neutrino oscillation parameters—the mass-squared difference  $\Delta m_{\text{atm}}^2$  and the mixing angle  $\theta_{\text{atm}}$  [55]:

$$2.0 (1.5) \times 10^{-3} \text{ eV}^2 \leq |\Delta m_{\text{atm}}^2| \leq 6.5 (8.0) \times 10^{-3} \text{ eV}^2, \quad (6)$$

$$0.87 (0.75) \leq \sin^2(2\theta_{\text{atm}}) \leq 1. \quad (7)$$

The sign of  $\Delta m_{\text{atm}}^2$  is undetermined by the data. The best fit value of  $|\Delta m_{\text{atm}}^2|$  found in [55] is  $|\Delta m_{\text{atm}}^2|_{\text{BF}} = 3.2 \times 10^{-3} \text{ eV}^2$ .

Global neutrino oscillation analyses of the most recent solar neutrino data [2,4,5,7,8] were performed, e.g., in Refs. [7,56–58]. The new high-precision Super-Kamiokande results [7] on the spectrum of recoil electrons and on the day-night (D-N) effect were included in the analyses. In Refs. [7,56,57] the solar neutrino data were analyzed in terms of the hypothesis of two-neutrino oscillations of solar neutrinos, characterized by the two parameters  $\Delta m_{\odot}^2 > 0$  and  $\theta_{\odot}$  (or  $\tan^2 \theta_{\odot}$ ). In Ref. [58] a three-neutrino oscillation analysis was performed (see further). The regions of the LMA MSW, SMA MSW (see, e.g., [59,60]), LOW and QVO solutions of the solar neutrino problem (see, e.g., [56]) allowed by the data at a given C.L. were determined. The studies performed in Refs. [7,56,57] showed, in particular, that (i) a relatively large part of the previously allowed region of the SMA MSW  $\nu_e \rightarrow \nu_{\mu(\tau)}$  transition solution is ruled out by the Super-Kamiokande data on the recoil- $e^-$  spectrum and the D-N effect, (ii) the LMA MSW  $\nu_e \rightarrow \nu_{\mu(\tau)}$  transition solution provides a better description of the data than the SMA MSW solution, and (iii) the purely VO solution due to the  $\nu_e \leftrightarrow \nu_{\mu(\tau)}$  oscillations (see, e.g., [61,62]) as well as the VO

<sup>3</sup>Let us note that the most recent solar neutrino data from the Super-Kamiokande experiment favor the LMA MSW solution of the solar neutrino problem.

TABLE I. Values of  $\Delta m_{\odot}^2$  obtained in the analyses of the solar neutrino data in Refs. [7,56,58] and used in the present study (see text for details). The best fit values (B.F.V.) in the different solution regions are also given.

		$\Delta m_{\odot}^2$ [eV <sup>2</sup> ]	B.F.V. [eV <sup>2</sup> ]
Ref. [7] (95% C.L.)	LMA	$2.5 \times 10^{-5} - 1.3 \times 10^{-4}$	$4.0 \times 10^{-5}$
	LOW-QVO	$5.6 \times 10^{-8} - 2.0 \times 10^{-7}$	
Ref. [56] [90% (99%) C.L.]	LMA	$1.6(1.6) \times 10^{-5} - 1.0(1.0) \times 10^{-4}$	$4.8 \times 10^{-5}$
	SMA	$(4.0 \times 10^{-6} - 1.0 \times 10^{-5})$	$8.0 \times 10^{-6}$
	LOW-QVO	$5.5(0.4) \times 10^{-9} - 1.4(2.4) \times 10^{-8}$	$1.0 \times 10^{-9}$
Ref. [58] [90% (99%) C.L.]	LMA	$1.6(1.5) \times 10^{-5} - 2.0(2.0) \times 10^{-4}$	$3.5 \times 10^{-5}$
	SMA	$4.0(3.0) \times 10^{-6} - 9.0(10.0) \times 10^{-6}$	
	LOW-QVO	$8.0(5.0) \times 10^{-10} - 3.0(4.0) \times 10^{-7}$	

and MSW solutions with solar  $\nu_e$  transitions into a sterile neutrino (see e.g., [63]),  $\nu_s$ , are strongly disfavored (if not ruled out) by the data. The Super-Kamiokande Collaboration, using a method of analysis which is different from those employed in Refs. [56,57], rules out the SMA MSW  $\nu_e \rightarrow \nu_{\mu(\tau)}$  transition solution at 95% C.L. In Tables I and II we give the results for the different solution regions derived in the two-neutrino  $\nu_e \rightarrow \nu_{\mu(\tau)}$  transition/oscillation analyses in Refs. [7,56]. The Super-Kamiokande Collaboration [7] did not produce 99% C.L. results, so we quote and use only their 95% C.L. allowed regions.

Very important constraints on the oscillations of electron (anti)neutrinos were obtained in the CHOOZ and Palo Verde disappearance experiments with reactor  $\bar{\nu}_e$  [64,65]. This experiment was sensitive to values of  $\Delta m^2 \geq 10^{-3}$  eV<sup>2</sup>, which includes the corresponding atmospheric neutrino region, Eq. (5). No disappearance of the reactor  $\bar{\nu}_e$  was observed. Performing a two-neutrino oscillation analysis, the following rather stringent upper bound on the value of the corresponding mixing angle  $\theta$  was obtained by the CHOOZ Collaboration<sup>4</sup> at 95% C.L. for  $\Delta m^2 \geq 1.5 \times 10^{-3}$  eV<sup>2</sup>:

$$\sin^2 \theta < 0.09. \quad (8)$$

The precise upper limit in Eq. (8) is  $\Delta m^2$  dependent. More concretely, it is a decreasing function of  $\Delta m^2$  as  $\Delta m^2$  increases up to  $\Delta m^2 \approx 6 \times 10^{-3}$  eV<sup>2</sup> with a minimum value  $\sin^2 \theta \approx 1 \times 10^{-2}$ . The upper limit becomes an increasing function of  $\Delta m^2$  when the latter increases further up to  $\Delta m^2 \approx 8 \times 10^{-3}$  eV<sup>2</sup>, where  $\sin^2 \theta < 2 \times 10^{-2}$ . Let us note that this dependence is accounted for, whenever necessary, in our analysis. The sensitivity to the value of the parameter  $\sin^2 \theta$  is expected to be considerably improved by the MINOS experiment [13] in which the following upper limit can be reached:

$$\sin^2 \theta < 5 \times 10^{-3}. \quad (9)$$

<sup>4</sup>The possibility of large  $\sin^2 \theta > 0.9$ , which is admitted by the CHOOZ data alone, is incompatible with the neutrino oscillation interpretation of the solar neutrino deficit (see, e.g., [36,37,60,47]). Let us note also that the CHOOZ limit does not depend on the sign of  $\Delta m^2$ : we have assumed that  $\Delta m^2 > 0$  for convenience.

As we have already mentioned, a comprehensive three-flavor neutrino oscillation analysis of the most recent solar neutrino, atmospheric neutrino, and CHOOZ data has recently been performed in Ref. [58]. The analysis was done under the assumption  $\Delta m_{\odot}^2 \ll |\Delta m_{\text{atm}}^2|$ , suggested by the results of the two-neutrino oscillation studies [7,56,57]. As follows from Eq. (5), the indicated inequality holds for

$$\Delta m_{\odot}^2 \lesssim 2.0 \times 10^{-4} \text{ eV}^2, \quad (10)$$

i.e., for the SMA MSW and LOW-QVO solutions and in most of the LMA MSW solution region found in [7,56,57] (see Table I). Under the condition  $\Delta m_{\odot}^2 \ll |\Delta m_{\text{atm}}^2|$ , the solar neutrino data constrain the parameters  $\Delta m_{\odot}^2$ ,  $\theta_{\odot}$ , and  $\theta$  (see, e.g., [47,60] and references quoted therein). It was found in Ref. [58] that the LMA MSW, SMA MSW, and LOW-QVO solutions of the solar neutrino problem are allowed and the corresponding solution regions were determined. The best fit point was found to lie in the LMA MSW solution region. Although the latter extends to values of  $\Delta m_{\odot}^2 \sim (7.0 - 8.0) \times 10^{-4}$  eV<sup>2</sup>, for  $\Delta m_{\odot}^2$  exceeding the upper bound in Eq. (10) the reliability (accuracy) of the results thus derived is questionable. For this reason in our further analysis we will use as a maximal value of  $\Delta m_{\odot}^2$  for the LMA MSW solution the value given in (10), which is reflected in Table I (see below). The atmospheric neutrino data analysis restricts in the case of  $\Delta m_{\odot}^2 \ll |\Delta m_{\text{atm}}^2|$  the mass-squared difference  $|\Delta m_{\text{atm}}^2|$  and the angles  $\theta_{\text{atm}}$  and  $\theta$  (see, e.g., [47,60]). The parameter  $\Delta m_{\text{atm}}^2$  is found in [58] to lie at 90% (99%) C.L. in the following interval:

$$1.4(1.1) \times 10^{-3} \text{ eV}^2 \leq |\Delta m_{\text{atm}}^2| \leq 6.1(7.3) \times 10^{-3} \text{ eV}^2, \quad (11)$$

with the best fit value given by  $|\Delta m_{\text{atm}}^2|_{\text{BF}} = 3.1 \times 10^{-3}$  eV<sup>2</sup>. Note that the upper and the lower limits in Eq. (11) depend on the value of  $\sin^2 \theta$ . More specifically, the upper bound is a decreasing function, while the lower one is an increasing function of  $\sin^2 \theta$  and the two bounds reach a common value at  $|\Delta m_{\text{atm}}^2| = 2.0 \times 10^{-3}$  eV<sup>2</sup> for  $\sin^2 \theta = 0.04$  (0.08) at 90% (99%) C.L. Combining all the bounds it is possible to constrain further the value of  $\theta$ . The result at 90% (99%) C.L. reads [58]

TABLE II. Values of  $\theta_\odot$  obtained in the analyses of the solar neutrino data in Refs. [7,56,58] and used in the present study.

		$\tan^2 \theta_\odot$	B.F.V.
Ref. [7] (95% C.L.)	LMA	0.21–0.67	0.38
	LOW-QVO	0.3–0.5	
Ref. [56] [90% (99%) C.L.]	LMA	0.20(0.19)–0.6(1.0)	0.35
	SMA	$(1.2 \times 10^{-4} - 1.8 \times 10^{-3})$	$6.0 \times 10^{-4}$
	LOW-QVO	0.57(0.42)–0.90(3.0)	0.70
Ref. [58] [90% (99%) C.L.]	LMA	0.18(0.16)–1.0(4.0)	0.35
	SMA	$2.0(1.0) \times 10^{-4} - 2.0(2.5) \times 10^{-3}$	
	LOW-QVO	0.4(0.2)–3.0(4.0)	

$$\sin^2 \theta < 0.05 \quad (0.08). \quad (12)$$

$$m_{\nu_e} < 2.5 \text{ eV} [67], \quad m_{\nu_e} < 2.9 \text{ eV} [68]. \quad (13)$$

The best fit value of  $\sin^2 \theta$  was found to be [58]  $\sin^2 \theta_{\text{BF}} = 0.005$ . The allowed regions for the different parameters can be read from the plots reported in [58] and are given in Tables I and II. We point out that, in general, the various bounds are correlated and such interdependences, whenever relevant, have been taken into account in our analysis.

In the next few years constraints on the values of  $\Delta m_{\odot}^2$ ,  $\theta_\odot$ ,  $\Delta m_{\text{atm}}^2$ ,  $\theta_{\text{atm}}$ , and  $\theta$  will be improved due to an increase of the statistics of the currently running experiments (e.g., SAGE, GNO, Super-Kamiokande, SNO, K2K) and an upgrade of some of them, as well as due to data from the new experiments BOREXINO, KamLand, MINOS, and CNGS. Hopefully, this will lead, for instance, to identification of a unique solution of the solar neutrino problem instead of the three solutions allowed by the current data.

Let us note that if three-flavor-neutrino mixing takes place, it would be possible to determine the sign of  $\Delta m_{\text{atm}}^2$ , e.g., by studying the transitions  $\nu_\mu \rightarrow \nu_e$  ( $\nu_e \rightarrow \nu_\mu$ ) and  $\bar{\nu}_\mu \rightarrow \bar{\nu}_e$  ( $\bar{\nu}_e \rightarrow \bar{\nu}_\mu$ ) in the Earth under the condition that the Earth matter effects be non-negligible [66]. A negative  $\Delta m_{\text{atm}}^2$  would correspond to a neutrino mass spectrum with inverted hierarchy or to three quasidegenerate neutrinos. In the inverted mass hierarchy case we adapt the notations so as to have  $\Delta m_{\text{atm}}^2 > 0$ . This leads to a different correspondence between  $\theta_\odot$ ,  $\theta_{\text{atm}}$ , and  $\theta$  and the elements of the neutrino mixing matrix in comparison with the case of a hierarchical neutrino mass spectrum. For the quasidegenerate neutrino mass spectrum which is considered in Sec. VI, the formulas corresponding to the case of  $\Delta m_{\text{atm}}^2 < 0$  can be obtained from those given in Sec. VI and corresponding to  $\Delta m_{\text{atm}}^2 > 0$ , by replacing  $\Delta m_{\text{atm}}^2$  with  $|\Delta m_{\text{atm}}^2|$ . In what regards  $(\beta\beta)_{0\nu}$  decay, under the condition  $\Delta m_{\odot}^2 \ll |\Delta m_{\text{atm}}^2|$  the results in the two cases coincide.

The Troitzk [67] and Mainz [68]  ${}^3\text{H}$   $\beta$ -decay experiments, studying the electron spectrum, provide information on the electron (anti)neutrino mass  $m_{\nu_e}$ . The data contain features which require further investigation (e.g., a peak in the end-point region which varies with time [67]). The upper bounds given by the authors (at 95% C.L.) read

There are prospects to increase the sensitivity of the  ${}^3\text{H}$   $\beta$ -decay experiments and probe the region of values of  $m_{\nu_e}$  down to  $m_{\nu_e} \sim (0.3-0.4) \text{ eV}$  [69].

Cosmological and astrophysical data provide information on the sum of the neutrino masses. The current upper bound reads (see, e.g., [70] and references quoted therein)

$$\sum_j m_j \lesssim 5.5 \text{ eV}. \quad (14)$$

The future experiments Microwave Anisotropy Probe (MAP) and Planck can be sensitive to [71]

$$\sum_j m_j \cong 0.4 \text{ eV}. \quad (15)$$

In the next sections we show that the data from a new generation of  $(\beta\beta)_{0\nu}$ -decay experiments, which will be sensitive to values of  $|\langle m \rangle| \gtrsim (0.01-0.10) \text{ eV}$ , can provide unique information on the neutrino mass spectrum as well as on the  $CP$  violation in the lepton sector in the case of massive Majorana neutrinos.

### III. FORMALISM OF NEUTRINO MIXING AND $(\beta\beta)_{0\nu}$ DECAY

The explanation of the atmospheric and solar neutrino data in terms of neutrino oscillations requires the existence of mixing of the three left-handed flavor neutrino fields  $\nu_{lL}$ ,  $l = e, \mu, \tau$ , in the weak charged lepton current:

$$\nu_{lL} = \sum_{j=1}^3 U_{lj} \nu_{jL}, \quad (16)$$

where  $\nu_{jL}$  is the left-handed field of the neutrino  $\nu_j$  having a mass  $m_j$  and  $U$  is a  $3 \times 3$  unitary mixing matrix—the lepton mixing matrix. We will assume that the neutrinos  $\nu_j$  are Majorana particles whose fields satisfy the Majorana condition

$$C(\bar{\nu}_j)^T = \nu_j, \quad j = 1, 2, 3, \quad (17)$$

where  $C$  is the charge conjugation matrix. We will also assume (without loss of generality) that  $m_1 < m_2 < m_3$ . One of the standard parametrizations of the matrix  $U$  reads

$$U = \begin{pmatrix} c_{12}c_{13} & s_{12}c_{13} & s_{13} \\ -s_{12}c_{23} - c_{12}s_{23}s_{13}e^{i\delta} & -c_{12}c_{23} - s_{12}s_{23}s_{13}e^{i\delta} & s_{23}c_{13}e^{i\delta} \\ s_{12}s_{23} - c_{12}c_{23}s_{13}e^{i\delta} & -c_{12}s_{23} - s_{12}c_{23}s_{13}e^{i\delta} & c_{23}c_{13}e^{i\delta} \end{pmatrix} \text{diag}(1, e^{i\alpha_{21}/2}, e^{i\alpha_{31}/2}), \quad (18)$$

where  $c_{ij} \equiv \cos \theta_{ij}$ ,  $s_{ij} \equiv \sin \theta_{ij}$ ,  $0 \leq \theta_{ij} \leq \pi/2$ ,  $\delta$  is the so-called Dirac  $CP$ -violating phase, and  $\alpha_{21}$  and  $\alpha_{31}$  are the Majorana  $CP$ -violating phases [23] (see also, e.g., [20]).

We are interested in the effective Majorana mass parameter (see Fig. 1)

$$|\langle m \rangle| \equiv |m_1 U_{e1}^2 + m_2 U_{e2}^2 + m_3 U_{e3}^2|, \quad (19)$$

whose value is determined by the values of the neutrino masses  $m_j$  and by the elements of the first row of the lepton mixing matrix  $U_{ej}$ . The latter satisfy the unitarity condition

$$\sum_{j=1}^3 |U_{ej}|^2 = 1. \quad (20)$$

We have

$$U_{ej} = |U_{ej}| e^{i\alpha_j/2}, \quad (21)$$

where  $\alpha_j$ ,  $j=1,2,3$ , are three phases. Only the phase differences  $(\alpha_j - \alpha_k) \equiv \alpha_{jk}$  ( $j > k$ ) can play a physical role. The mixing matrix in Eq. (18) is written taking this into account.

In the general case, one can have

$$C(\bar{\nu}_j)^T = (\xi_j^*)^2 \nu_j, \quad j=1,2,3, \quad (22)$$

where  $\xi_j$ ,  $j=1,2,3$ , are three phases. Only two combinations of the six phases  $\alpha_j$  and  $\xi_j$  represent physical Majorana  $CP$ -violating phases. The effective Majorana mass parameter now has the form

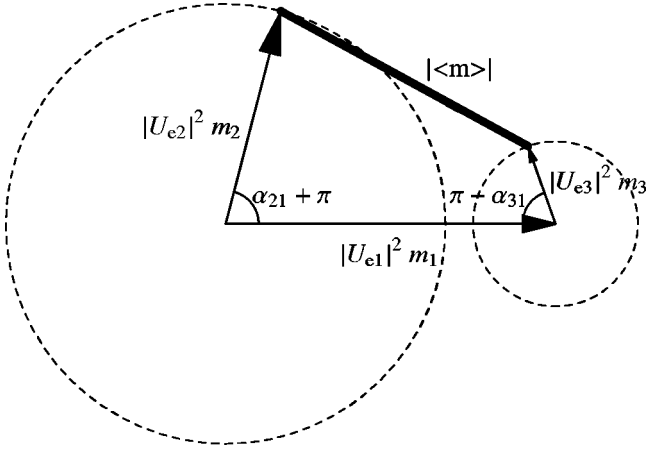


FIG. 1. The effective Majorana mass  $|\langle m \rangle|$  represented as the absolute value of the vector sum of the three contributions in Eq. (19) using Eq. (21), each of which is expressed as a vector in the complex plane (see Sec. VI for details). The  $CP$ -violating phases  $\alpha_{21}$  and  $\alpha_{31}$  shown in the figure can vary between 0 and  $2\pi$ .

$$|\langle m \rangle| \equiv |m_1 U_{e1}^2 \xi_1^2 + m_2 U_{e2}^2 \xi_2^2 + m_3 U_{e3}^2 \xi_3^2|. \quad (23)$$

Obviously, the two physical Majorana  $CP$ -violating phases on which  $|\langle m \rangle|$  depends are  $\alpha_{21} \equiv \arg(U_{e2}^2 \xi_2^2) - \arg(U_{e1}^2 \xi_1^2)$  and  $\alpha_{31} \equiv \arg(U_{e3}^2 \xi_3^2) - \arg(U_{e1}^2 \xi_1^2)$ . Actually, all  $CP$ -violation effects associated with the Majorana nature of the massive neutrinos are generated by  $\alpha_{21} \neq k\pi$  and  $\alpha_{31} \neq k'\pi$ ,  $k, k' = 0, 1, 2, \dots$ . Indeed, under a rephasing of the charged lepton,  $l(x)$ , and the neutrino,  $\nu_j(x)$ , fields in the weak charged lepton current,  $l(x) \rightarrow e^{i\eta_l} l(x)$  and  $\nu_j(x) \rightarrow e^{i\beta_j} \nu_j(x)$ , the elements of the lepton mixing matrix, and the phase factors in the Majorana condition for the Majorana neutrino fields change as follows:

$$U_{lj} \rightarrow U_{lj} e^{-i(\eta_l - \beta_j)}, \quad l = e, \mu, \tau, \quad j = 1, 2, 3, \quad (24)$$

$$\xi_j \rightarrow \xi_j e^{-i\beta_j}. \quad (25)$$

As was shown in [39], in the lepton sector of the theory under discussion with mixing of three massive Majorana neutrinos there exist three rephasing invariants. The first is the standard Dirac one,  $J$ , present in the case of mixing of three massive Dirac neutrinos [72,39] (see also [73]):

$$J = \text{Im}(U_{\mu 2} U_{e 3} U_{\mu 3}^* U_{e 2}^*). \quad (26)$$

The existence of the other two  $S_1$  and  $S_2$  is related to the Majorana nature of the massive neutrinos  $\nu_j$  [39]:

$$S_1 \equiv \text{Im}(U_{e 1} U_{e 3}^* \xi_3^* \xi_1), \quad (27)$$

$$S_2 \equiv \text{Im}(U_{e 2} U_{e 3}^* \xi_3^* \xi_2). \quad (28)$$

A geometrical representation of  $CP$  violation in the lepton sector in terms of unitarity triangles in the case of three-neutrino mixing and presence of Majorana  $CP$ -violating phases in the lepton mixing matrix is given in [41]. The two Majorana  $CP$ -violating phases  $\alpha_{21}$  and  $\alpha_{31}$  are determined by the two independent rephasing invariants  $S_{1,2}$ . We have

$$\cos \alpha_{31} = 1 - 2 \frac{S_1^2}{|U_{e1}|^2 |U_{e3}|^2}, \quad (29)$$

$$\cos(\alpha_{31} - \alpha_{21}) = \cos(\alpha_3 - \alpha_2) = 1 - 2 \frac{S_2^2}{|U_{e2}|^2 |U_{e3}|^2}, \quad (30)$$

and

$$\begin{aligned} \cos \alpha_{21} &= \cos(\alpha_{31} - \alpha_{21}) \cos \alpha_{31} \\ &+ \sin(\alpha_{31} - \alpha_{21}) \sin \alpha_{31}. \end{aligned} \quad (31)$$

One can express  $|\langle m \rangle|$  in terms of rephasing-invariant quantities as

$$\begin{aligned} |\langle m \rangle|^2 = & m_1^2 |U_{e1}|^4 + m_2^2 |U_{e2}|^4 + m_3^2 |U_{e3}|^4 \\ & + 2m_1 m_2 |U_{e1}|^2 |U_{e2}|^2 \cos \alpha_{21} \\ & + 2m_1 m_3 |U_{e1}|^2 |U_{e3}|^2 \cos \alpha_{31} \\ & + 2m_2 m_3 |U_{e2}|^2 |U_{e3}|^2 \cos(\alpha_{31} - \alpha_{21}). \end{aligned} \quad (32)$$

Note that  $|\langle m \rangle|$  depends only on  $S_{1,2}$  and does not depend on the Dirac rephasing invariant  $J$ . This is a consequence of the specific choice of the rephasing invariants  $S_{1,2}$ , Eq. (28), which is not unique [39]. With this choice the amplitude of the  $K^+ \rightarrow \pi^- + \mu^+ + \mu^+$  decay, for instance, which, as like the  $(\beta\beta)_{0\nu}$  decay, is generated by the exchange of the three virtual massive Majorana neutrinos in the scheme under discussion, depends, as can be shown, on all three rephasing invariants  $S_1$ ,  $S_2$ , and  $J$ .

If  $CP$  invariance holds in the lepton sector, we have, in particular,  $S_1 = 0$  or  $\text{Re}(U_{e1} U_{e3}^* \xi_3^* \xi_1) = 0$ , and  $S_2 = 0$  or  $\text{Re}(U_{e2} U_{e3}^* \xi_3^* \xi_2) = 0$ . In this case the unitarity triangles reduce to lines oriented either along the horizontal or the vertical axis on the plane [41]. In terms of constraints on the phases  $\alpha_{21}$  and  $\alpha_{31}$  this implies  $\alpha_{21} = k\pi$ ,  $\alpha_{31} = k'\pi$  with  $k, k' = 0, 1, 2, \dots$ .

In all our subsequent analyses we will set for convenience (and without loss of generality)  $\xi_j = 1$ ,  $j = 1, 2, 3$ ; i.e., we will assume that the fields of the Majorana neutrinos  $\nu_j$  satisfy the Majorana conditions (17). In this case  $\alpha_{21} = \alpha_2 - \alpha_1$  and  $\alpha_{31} = \alpha_3 - \alpha_1$ , where  $\alpha_j$  are determined by Eq. (21). The  $CP$ -invariance constraint on the elements of the lepton mixing matrix of interest reads<sup>5</sup> [74,75] (see also [20])

$$U_{ej}^* = \eta_j^{CP} U_{ej}, \quad (33)$$

where  $\eta_j^{CP} = i\phi_j = \pm i$  is the  $CP$  parity of the Majorana neutrino  $\nu_j$  with mass  $m_j > 0$ . In this case  $|\langle m \rangle|$  is given by

$$|\langle m \rangle| \equiv \left| \sum_{j=1}^3 \eta_j^{CP} |U_{ej}|^2 m_j \right| = \left| \sum_{j=1}^3 \phi_j |U_{ej}|^2 m_j \right|. \quad (34)$$

For establishing a direct relation with the mixing angles constrained by the solar neutrino data and the data from the CHOOZ experiment, it proves convenient to express (e.g., in the case of neutrino mass hierarchy)  $|U_{e1}|$  and  $|U_{e2}|$  in the form

$$|U_{e1}| = \cos \varphi \sqrt{1 - |U_{e3}|^2}, \quad |U_{e2}| = \sin \varphi \sqrt{1 - |U_{e3}|^2}, \quad (35)$$

where  $\varphi$  is an angle and we have used the relation  $|U_{e1}|^2 + |U_{e2}|^2 = 1 - |U_{e3}|^2$ . In certain cases (e.g., inverted neutrino

mass hierarchy) the analogous relations  $|U_{e2}| = \cos \tilde{\varphi} \sqrt{1 - |U_{e1}|^2}$ ,  $|U_{e3}| = \sin \tilde{\varphi} \sqrt{1 - |U_{e1}|^2}$  are more useful. Depending on the type of neutrino mass spectrum, we will have either  $\varphi = \theta_\odot$ ,  $|U_{e3}|^2 = \sin^2 \theta$ , or  $\tilde{\varphi} = \theta_\odot$ ,  $|U_{e1}|^2 = \sin^2 \theta$ .

The neutrino oscillation experiments, as is well known, provide information on  $\Delta m_{jk}^2 = m_j^2 - m_k^2$  ( $j > k$ ). In the case of three-neutrino mixing, Eq. (16), there are two independent  $\Delta m^2$  parameters:  $\Delta m_{31}^2$ , for instance, can be expressed as  $\Delta m_{31}^2 = \Delta m_{32}^2 + \Delta m_{21}^2$ . Correspondingly, as an independent set of three neutrino mass parameters we can choose  $m_1$ ,  $\sqrt{\Delta m_{21}^2}$ , and  $\sqrt{\Delta m_{32}^2}$ . We have

$$m_2 = \sqrt{m_1^2 + \Delta m_{21}^2}, \quad (36)$$

$$m_3 = \sqrt{m_1^2 + \Delta m_{21}^2 + \Delta m_{32}^2}. \quad (37)$$

The mass-squared difference inferred from a neutrino oscillation interpretation of the atmospheric neutrino data,  $\Delta m_{\text{atm}}^2$ , is equal to  $\Delta m_{31}^2$ ,

$$\Delta m_{\text{atm}}^2 = \Delta m_{31}^2 = \Delta m_{21}^2 + \Delta m_{32}^2, \quad (38)$$

while for the one deduced from the solar neutrino data,  $\Delta m_\odot^2$ , we have two possibilities

$$\Delta m_\odot^2 \equiv \Delta m_{32}^2 \quad \text{or} \quad \Delta m_\odot^2 \equiv \Delta m_{21}^2. \quad (39)$$

Depending on the relative magnitudes of  $m_1$ ,  $\sqrt{\Delta m_{21}^2}$ , and  $\sqrt{\Delta m_{32}^2}$ , one recovers the different possible types of neutrino mass spectrum:

(1) If  $m_1 \ll \sqrt{\Delta m_{21}^2} \ll \sqrt{\Delta m_{32}^2}$ , one has  $m_1 \ll m_2 \ll m_3$ , i.e., hierarchical neutrino mass spectrum.

(2)  $m_1 \ll \sqrt{\Delta m_{32}^2} \ll \sqrt{\Delta m_{21}^2}$  implies  $m_1 \ll m_2 \approx m_3$ , i.e., neutrino mass spectrum with inverted hierarchy.

(3) For  $\sqrt{\Delta m_{21}^2}, \sqrt{\Delta m_{32}^2} \ll m_1$ , we have  $m_1 \approx m_2 \approx m_3$ , i.e., quasidegenerate neutrino mass spectrum.

(4) If  $\sqrt{\Delta m_{21}^2} \ll \sqrt{\Delta m_{32}^2} \sim O(m_1)$ , one finds  $m_1 \approx m_2 < m_3$ , i.e., spectrum with ‘‘partial mass hierarchy.’’ This pattern of neutrino masses interpolates between the hierarchical one and the quasidegenerate one.

(5) For  $\sqrt{\Delta m_{32}^2} \ll \sqrt{\Delta m_{21}^2} \sim O(m_1)$ , we have  $m_1 < m_2 \approx m_3$ , i.e., spectrum with ‘‘partial inverted mass hierarchy.’’ This pattern interpolates between the inverted mass hierarchy spectrum and the quasidegenerate one.

For each of the possible patterns of neutrino masses indicated above, we will study in detail the implications of the data on neutrino oscillations, obtained in the experiments with solar and atmospheric neutrinos and in the CHOOZ experiment, for the searches of  $(\beta\beta)_{0\nu}$  decay.

#### IV. HIERARCHICAL NEUTRINO MASS SPECTRUM

The hierarchical neutrino mass spectrum is characterized by the following pattern of the neutrino masses  $m_j$ :

$$m_1 \ll m_2 \ll m_3. \quad (40)$$

<sup>5</sup>This constraint is obtained from the requirement of  $CP$  invariance of the charged current weak interaction Lagrangian  $\mathcal{L}^{cc}$ , by choosing the arbitrary phase factors in the  $CP$  transformation laws of the electron and the  $W$ -boson fields equal to 1.

This type of neutrino mass spectrum is predicted by the standard versions of the seesaw mechanism of neutrino mass generation [22]. The pattern corresponds to the inequalities<sup>6</sup>

$$m_1 \ll \sqrt{\Delta m_{21}^2} \ll \sqrt{\Delta m_{32}^2}. \quad (41)$$

Using Eqs. (40) and (41) it is possible to make the identification (see, e.g., [47,60])

$$\begin{aligned} \Delta m_{\odot}^2 &\equiv \Delta m_{21}^2, & \Delta m_{\text{atm}}^2 &\equiv \Delta m_{32}^2, \\ |U_{e1}|^2 &= \cos^2 \theta_{\odot} (1 - |U_{e3}|^2), \\ |U_{e2}|^2 &= \sin^2 \theta_{\odot} (1 - |U_{e3}|^2), \\ |U_{e3}|^2 &\equiv \sin^2 \theta < 0.09 \quad (\text{CHOOZ}). \end{aligned} \quad (42)$$

We will suppose that  $\Delta m_{\text{atm}}^2$  lies in the interval (5) or (11), that  $\Delta m_{\odot}^2$  and  $\theta_{\odot}$  take values in the regions given in Tables I and II, and that  $|U_{e3}|^2$  satisfies the CHOOZ upper bound. Equations (40) and (42) further imply

$$m_2 \simeq \sqrt{\Delta m_{\odot}^2}, \quad m_3 \simeq \sqrt{\Delta m_{\text{atm}}^2}. \quad (43)$$

Using Eqs. (19), (21), (42), and (43) we can express the effective Majorana mass parameter in terms of the quantities whose values are determined in the solar and atmospheric neutrino experiments, and of the phase  $(\alpha_3 - \alpha_2)$ :

$$\begin{aligned} |\langle m \rangle| &\simeq \sqrt{\Delta m_{\odot}^2} (1 - |U_{e3}|^2) \sin^2 \theta_{\odot} \\ &+ \sqrt{\Delta m_{\text{atm}}^2} |U_{e3}|^2 e^{i(\alpha_3 - \alpha_2)}, \end{aligned} \quad (44)$$

where the phases  $\alpha_{2,3}$  are determined by Eq. (21) and we have neglected the contribution of the term  $\sim m_1$ . Note that although in this case one of three massive Majorana neutrinos effectively ‘‘decouples’’ and does not give a contribution to  $|\langle m \rangle|$ , the value of  $|\langle m \rangle|$  still depends on the Majorana  $CP$ -violating phase  $\alpha_{32} = \alpha_3 - \alpha_2$ . This reflects the fact that in contrast to the case of massive Dirac neutrinos (or quarks),  $CP$  violation can take place in the mixing of only two massive Majorana neutrinos [23].

As a result of the presence of the first term in Eq. (44), one obtains different predictions for  $|\langle m \rangle|$  for the LMA, SMA, and LOW-QVO solutions of the solar neutrino problem, as the three solutions require different ranges of values of  $\sin^2 \theta_{\odot}$  and  $\Delta m_{\odot}^2$ .

Consider first the case of  $CP$  conservation. There exist two possibilities.

*Case A.* The neutrinos  $\nu_2$  and  $\nu_3$  can have the same  $CP$  parities, i.e.,  $\phi_2 = \phi_3$ . In this case (with the phase conventions we are using; see Sec. III)  $\alpha_{32} \equiv \alpha_3 - \alpha_2 = 0$  (or  $\alpha_{21} = \alpha_{31} = 0, \pm \pi$ ), and the effective Majorana mass  $|\langle m \rangle|$  is given by

$$|\langle m \rangle| \simeq \sqrt{\Delta m_{\odot}^2} \sin^2 \theta_{\odot} (1 - |U_{e3}|^2) + \sqrt{\Delta m_{\text{atm}}^2} |U_{e3}|^2. \quad (45)$$

Using the results on  $\Delta m_{\text{atm}}^2$ ,  $\Delta m_{\odot}^2$ ,  $\sin^2 \theta_{\odot}$ , and  $|U_{e3}|^2$  obtained in Ref. [58] at 90% (99%) C.L. (quoted in Sec. II and in Tables I and II), we find that in the cases of the LMA, SMA, and LOW-QVO solutions of the solar neutrino problem  $|\langle m \rangle|$  is bounded to lie in the following intervals:

$$6.1 (5.3) \times 10^{-4} \text{ eV} \leq |\langle m \rangle| \leq 7.4 (14) \times 10^{-3} \text{ eV}, \quad \text{LMA}, \quad (46)$$

$$2.0 (0.8) \times 10^{-7} \text{ eV} \leq |\langle m \rangle| \leq 1.9 (3.6) \times 10^{-3} \text{ eV}, \quad \text{SMA}, \quad (47)$$

$$6.7 (0.5) \times 10^{-5} \text{ eV} \leq |\langle m \rangle| \leq 3.5 (3.6) \times 10^{-3} \text{ eV}, \quad \text{LOW-QVO}. \quad (48)$$

For the values of the parameters providing the best fit of the solar and atmospheric neutrino data [58] one finds  $|\langle m \rangle|_{\text{BF}} = 1.8 \times 10^{-3} \text{ eV}$ . Note that in the case of the LMA solution,  $|\langle m \rangle|$  can reach  $|\langle m \rangle| \equiv (1-2) \times 10^{-2} \text{ eV}$ . If the LMA solution admits values of  $\Delta m_{\odot}^2 \sim (7-8) \times 10^{-4} \text{ eV}^2$ , as suggested in [58],  $|\langle m \rangle|$  can be as large as  $\sim 3 \times 10^{-2} \text{ eV}$ . This is the maximal value  $|\langle m \rangle|$  can have in the case of the hierarchical neutrino mass spectrum. Values of  $|\langle m \rangle| \geq 10^{-2} \text{ eV}$  can be tested in the next generation of  $(\beta\beta)_{0\nu}$ -decay experiments, as we have discussed in the Introduction.

The maximal allowed values of  $|\langle m \rangle|$ ,  $\max(|\langle m \rangle|)$ , in the case of the SMA and LOW-QVO solutions are by a factor of  $\sim (2-4)$  smaller than that for the LMA solution. This is related to the fact that for the SMA and LOW-QVO solutions

$$\max(|\langle m \rangle|) = \max(\sqrt{\Delta m_{\text{atm}}^2} |U_{e3}|^2), \quad (49)$$

while for the LMA solution  $\sqrt{\Delta m_{\odot}^2} \sin^2 \theta_{\odot}$  can be as large as  $\sim 1.1 \times 10^{-2} \text{ eV}$  and both terms in Eq. (44) contribute to  $\max(|\langle m \rangle|)$ .

The minimal allowed values of  $|\langle m \rangle|$ ,  $\min(|\langle m \rangle|)$ , given in Eqs. (46)–(48), are exceedingly small. Let us note nevertheless that for a given solution of the solar neutrino problem they correspond to  $m_1$  having a value much smaller than the  $\min(|\langle m \rangle|)$  in Eqs. (46)–(48), i.e., to  $m_1 \ll 7.0 \times 10^{-4} \text{ eV}$  for the LMA solution, etc. If, however,  $m_1 \ll \sqrt{\Delta m_{\odot}^2}$ , but  $m_1 |U_{e1}|^2 = m_1 (1 - |U_{e3}|^2) \cos^2 \theta_{\odot}$  is of the order of, or larger than, some of the  $\min(|\langle m \rangle|)$  given in Eqs. (46)–(48), the corresponding lower bounds will be modified. This can happen in the case of the SMA MSW solution, while  $\min(|\langle m \rangle|)$  for the LMA and LOW-QVO solutions are practically stable with respect to ‘‘finite’’  $m_1$  corrections. Indeed, for the LMA (LOW-QVO) solution,  $m_1 \ll \sqrt{\Delta m_{\odot}^2}$  implies  $m_1 \leq 4.0 (0.025) \times 10^{-4} \text{ eV}$  and thus  $m_1 |U_{e1}|^2 \leq 2.0 (0.013) \times 10^{-4} \text{ eV}$ , which can change the relevant values of  $\min(|\langle m \rangle|)$  in Eq. (46) [Eq. (48)] by not more than  $\sim 30\%$ . In contrast, in the case of the SMA solution for which  $\cos^2 \theta_{\odot} \equiv 1$ , the inequality  $m_1 \ll \sqrt{\Delta m_{\odot}^2}$  is satisfied for  $m_1 \leq 1.8 \times 10^{-4} \text{ eV}$ . Correspondingly,  $m_1 (1 - |U_{e3}|^2) \cos^2 \theta_{\odot}$

<sup>6</sup>The case of a neutrino mass spectrum with partial hierarchy  $m_1 \simeq m_2 < m_3$  will be treated in Sec. VII.



$\leq 1.8 \times 10^{-4}$  eV and  $\min(|\langle m \rangle|)$  can range from  $\sim 1.8 \times 10^{-4}$  eV to 0 eV. Let us note also that in the case of the SMA solution, a value of  $|\langle m \rangle| \geq 8.0 \times 10^{-4}$  eV would imply (for a hierarchical neutrino mass spectrum) that

$$\text{SMA, } |\langle m \rangle| \geq 8.0 \times 10^{-4} \text{ eV: } |\langle m \rangle| \approx \sqrt{\Delta m_{\text{atm}}^2} |U_{e3}|^2. \quad (50)$$

Using the results of the two-neutrino oscillation analyses of Refs. [7,56] (see Tables I and II), the results on  $\Delta m_{\text{atm}}^2$  from Ref. [55], Eq. (7), and the upper limit on  $|U_{e3}|^2$ , obtained in the CHOOZ experiment [64], we get the following intervals of possible values of  $|\langle m \rangle|$ :

$$\begin{aligned} 0.8 \times 10^{-3} \text{ eV} \leq |\langle m \rangle| \leq 7.6 \times 10^{-3} \text{ eV, } & \text{LMA [7,55,64],} \\ 5.0 \times 10^{-5} \text{ eV} \leq |\langle m \rangle| \leq 3.6 \times 10^{-3} \text{ eV,} & \\ & \text{LOW-QVO [7,55,64],} \end{aligned} \quad (51)$$

and

$$\begin{aligned} 6.7 (5.4) \times 10^{-4} \text{ eV} \leq |\langle m \rangle| \leq 7.4 (8.5) \times 10^{-3} \text{ eV,} & \\ & \text{LMA [55,56,64],} \\ (2.4 \times 10^{-7} \text{ eV} \leq |\langle m \rangle| \leq 4.0 \times 10^{-3} \text{ eV}), & \\ & \text{SMA [55,56,64],} \\ 2.7 (0.6) \times 10^{-5} \text{ eV} \leq |\langle m \rangle| \leq 3.5 (4.0) \times 10^{-3} \text{ eV,} & \\ & \text{LOW-QVO [55,56,64],} \end{aligned} \quad (52)$$

where the numbers (the numbers in brackets) correspond to the 90% (99%) C.L. solutions of the  $\nu_\odot$  problem in [56].

The values of  $\max(|\langle m \rangle|)$  for the LMA solution derived in the two-neutrino oscillation analyses [7,56] do not exceed  $8.5 \times 10^{-3}$  eV and are smaller than the corresponding one for the LMA solution obtained in the three-neutrino oscillation analysis [58]. This difference is due to the difference in the maximal allowed values of  $\sqrt{\Delta m_\odot^2} (1 - |U_{e3}|^2) \sin^2 \theta_\odot$  in the two cases. The minimal  $|\langle m \rangle|$  for the SMA solution in Eq. (52) is again unstable with respect to ‘‘finite’’  $m_1$  corrections and actually can have any value from  $\sim 10^{-4}$  eV to 0 eV.

*Case B.*  $\nu_2$  and  $\nu_3$  have opposite *CP* parities, i.e.,  $\phi_2 = -\phi_3$ . We have  $\alpha_{32} = \pm \pi$  (or  $\alpha_{21} = \alpha_{31} \pm \pi = 0, \pm \pi$ ), and the effective Majorana mass parameter is given by

$$|\langle m \rangle| = |\sqrt{\Delta m_\odot^2} \sin^2 \theta_\odot (1 - |U_{e3}|^2) - \sqrt{\Delta m_{\text{atm}}^2} |U_{e3}|^2|. \quad (53)$$

In this case there exists the possibility of cancellation [76] between the two terms in Eq. (53). Correspondingly, one can have  $|\langle m \rangle| = 0$  eV for all solutions of the solar neutrino problem.

The 90% (99%) C.L. results of the three-neutrino oscillation analysis of Ref. [58] imply the following ranges of allowed values of  $|\langle m \rangle|$ :

$$\begin{aligned} 0 \leq |\langle m \rangle| \leq 6.4 (10) \times 10^{-3} \text{ eV, } & \text{LMA,} \\ 0 \leq |\langle m \rangle| \leq 1.8 (3.1) \times 10^{-3} \text{ eV, } & \text{LOW-QVO,} \\ 0 \leq |\langle m \rangle| \leq 1.9 (3.5) \times 10^{-3} \text{ eV, } & \text{SMA.} \end{aligned} \quad (54)$$

To the best fit values of the parameters found in [58] (the best fit  $\Delta m_\odot^2$  and  $\sin^2 \theta_\odot$  lie in the LMA solution region), there corresponds  $|\langle m \rangle|_{\text{BF}} = 1.2 \times 10^{-3}$  eV.

The results of the two-neutrino oscillation analyses of Refs. [7] and [56] and of [55,64] lead to the following possible values of  $|\langle m \rangle|$ :

$$\begin{aligned} 0 \leq |\langle m \rangle| \leq 4.5 \times 10^{-3} \text{ eV, } & \text{LMA [7,55,64],} \\ 0 \leq |\langle m \rangle| \leq 3.5 \times 10^{-3} \text{ eV, } & \text{LOW-QVO [7,55,64],} \end{aligned} \quad (55)$$

and

$$\begin{aligned} 0 \leq |\langle m \rangle| \leq 3.7 (5.0) \times 10^{-3} \text{ eV, } & \text{LMA [55,56,64],} \\ (0 \leq |\langle m \rangle| \leq 4.0 \times 10^{-3} \text{ eV}), & \text{SMA [55,56,64],} \\ 0 \leq |\langle m \rangle| \leq 3.5 (4.0) \times 10^{-3} \text{ eV,} & \\ & \text{LOW-QVO [55,56,64].} \end{aligned} \quad (56)$$

We see that the 99% C.L. results of the three-neutrino oscillation analysis [58] allow values of  $\max(|\langle m \rangle|) \approx 10^{-2}$  eV for the LMA solution. Using the results of the two-neutrino oscillation analyses [7,55,56,64] one gets  $\max(|\langle m \rangle|) \leq 5.0 \times 10^{-3}$  eV.

The possibility of partial or complete cancellation between the two terms in Eq. (53) for  $|\langle m \rangle|$  is extremely important in view of future searches for  $(\beta\beta)_{0\nu}$  decay. Barring finite  $m_1$  corrections which can be relevant in the case of the SMA solution of the solar neutrino problem, the cancellation can take place if  $|U_{e3}|^2$  has a value given by

$$|\langle m \rangle| = 0: \quad |U_{e3}|_0^2 = \frac{\sqrt{\Delta m_\odot^2} \sin^2 \theta_\odot}{\sqrt{\Delta m_\odot^2} \sin^2 \theta_\odot + \sqrt{\Delta m_{\text{atm}}^2}}. \quad (57)$$

For the ranges of allowed values of  $\Delta m_\odot^2$ ,  $\sin^2 \theta_\odot$  for the three solutions of the  $\nu_\odot$  problem, and  $\Delta m_{\text{atm}}^2$ , found in [58], the corresponding values of  $|U_{e3}|_0^2$  for which the cancellation can occur belong to the intervals

$$\begin{aligned} 8.0 (8.0) \times 10^{-3} \leq |U_{e3}|_0^2 \leq 1.3 (3.7) \times 10^{-1}, & \text{LMA,} \\ 1.0 (0.3) \times 10^{-5} \leq |U_{e3}|_0^2 \leq 7.0 (20) \times 10^{-5}, & \text{SMA,} \\ 8.0 (0.7) \times 10^{-4} \leq |U_{e3}|_0^2 \leq 0.5 (13) \times 10^{-2}, & \text{LOW-QVO.} \end{aligned} \quad (58)$$

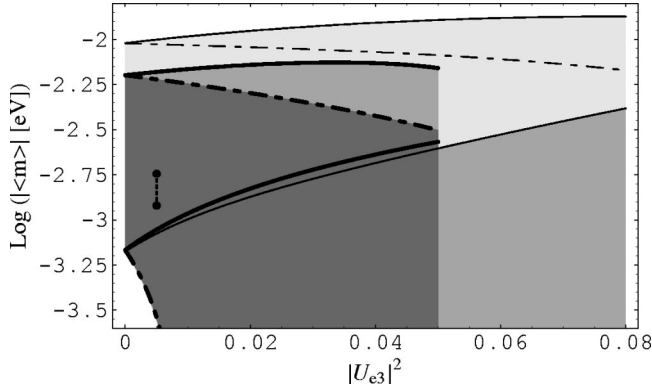


FIG. 2. The effective Majorana mass  $|\langle m \rangle|$ , allowed by the data from the solar and atmospheric neutrino and CHOOZ experiments, as a function of  $|U_{e3}|^2$  in the case of a hierarchical neutrino mass spectrum, Eq. (40). The values of  $|\langle m \rangle|$  are obtained for  $\Delta m_{\odot}^2$  and  $\sin^2 \theta_{\odot}$  from the LMA MSW solution region and  $\Delta m_{\text{atm}}^2$  and  $|U_{e3}|^2$  derived in [58] at 90% C.L. (medium gray and dark gray regions at  $|U_{e3}|^2 < 0.05$ ) and at 99% C.L. (light, medium, and dark gray regions at  $|U_{e3}|^2 < 0.08$ ). The 90% (99%) C.L. allowed regions located (i) between the two thick (thin) solid lines and (ii) between the thick (thin) dashed lines and the horizontal axis correspond to the two cases of  $CP$  conservation: (i)  $\phi_2 = \phi_3$  and (ii)  $\phi_2 = -\phi_3$ ,  $i\phi_{2,3}$  being the  $CP$  parities of  $\nu_{2,3}$ . The values of  $|\langle m \rangle|$ , calculated for the best fit values of the input parameters, are indicated by thick dots ( $CP$  conservation) and a dotted line ( $CP$  violation). In the case of  $CP$  violation all regions marked with different gray-color scales are allowed.

These regions for  $|U_{e3}|_0^2$  overlap with the experimentally allowed one and, as we noticed earlier, there can be a complete cancellation between the different contributions in  $|\langle m \rangle|$  for all solutions of the solar neutrino problem. Note, however, that the parameters entering into the expression (57) for  $|U_{e3}|_0^2$  are not related, in general, and therefore a complete cancellation of the terms in the expression for  $|\langle m \rangle|$  seems to require a fine-tuning or the existence of a specific symmetry (see, e.g., [76,77,20]). Note also that the cancellation cannot occur for the best fit value of  $|U_{e3}|^2 = 0.005$  (LMA) found in [58]. One arrives at analogous conclusions performing this analysis exploiting the two-neutrino oscillation results of Refs. [7,55,56,64].

The MINOS experiment [13] currently under preparation will be able to search for  $\nu_{\mu} \rightarrow \nu_e$  transitions and can probe values of  $|U_{e3}|^2 \geq 5 \times 10^{-3}$ . These data can provide information on the possibility of cancellation of the two terms in  $|\langle m \rangle|$  only for the case of the LMA solution of the solar neutrino problem. If it is found that  $|U_{e3}|^2 \geq 8 \times 10^{-3}$ , the two terms in Eq. (53) for  $|\langle m \rangle|$  can cancel and one can have  $|\langle m \rangle| \cong 0$  eV. If, on the other hand,  $|U_{e3}|^2 \leq 8 \times 10^{-3}$ , there

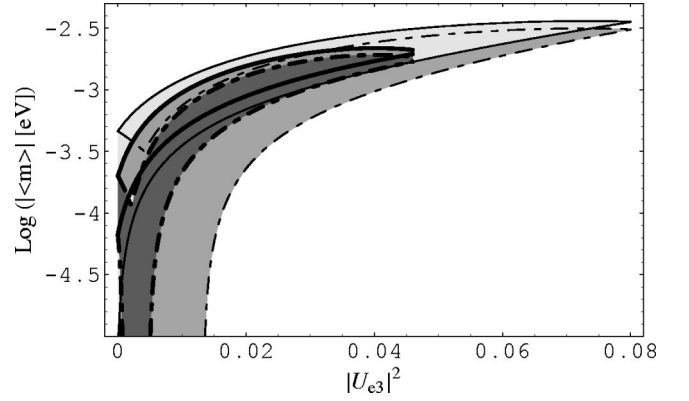


FIG. 3. The same as Fig. 2 but for  $\Delta m_{\odot}^2$  and  $\sin^2 \theta_{\odot}$  from the 90% (99%) C.L. region of the LOW-QVO solution of the  $\nu_{\odot}$  problem [58]. The regions delimited by the two thick (thin) solid and dashed lines correspond to the two cases of  $CP$  conservation: (i)  $\phi_2 = \phi_3$  (regions within the solid lines) and (ii)  $\phi_2 = -\phi_3$  (regions within the dashed lines). In the case of  $CP$  violation,  $(\alpha_3 - \alpha_2) \neq k\pi$ ,  $k=0,1,\dots$ , all regions marked by different gray-color scales are allowed.

cannot be a complete cancellation. However, the dominant contribution to  $|\langle m \rangle|$ , Eq. (53), would be given by the term  $\sqrt{\Delta m_{\odot}^2}(1 - |U_{e3}|^2)\sin^2 \theta_{\odot}$  and in this case  $|\langle m \rangle|$  would be relatively small:

$$|U_{e3}|^2 \leq 8 \times 10^{-3}: \quad |\langle m \rangle| \sim (\text{few} \times 10^{-4} - \text{few} \times 10^{-3}) \text{ eV}. \quad (59)$$

Our results are summarized in Figs. 2, 3, and 4 in which we show the allowed ranges of  $|\langle m \rangle|$  as a function of  $|U_{e3}|^2$  for the LMA, LOW-QVO, and SMA solutions, respectively, found in Ref. [58]. The figures are obtained for any possible values of the  $CP$ -violating phase  $(\alpha_3 - \alpha_2)$ . The regions of allowed values of  $|\langle m \rangle|$  in the cases of  $CP$  conservation ( $\phi_2 = \pm \phi_3$  or  $\alpha_3 - \alpha_2 = 0, \pm\pi$ ) cover completely that in the case of  $CP$  violation [ $(\alpha_3 - \alpha_2) \neq k\pi$ ,  $k=0,1,\dots$ ]. This is mainly due to uncertainties in the value of  $\Delta m_{\odot}^2$ . With improvement of the precision of  $\Delta m_{\odot}^2$  it will be possible to restrict the allowed ranges of values of  $|\langle m \rangle|$  in the indicated cases. The latter can lead to a separation between the allowed regions of  $|\langle m \rangle|$ , corresponding to the cases of  $CP$  conservation and of  $CP$  violation. Let us note also that the cancellation leading to  $|\langle m \rangle| \cong 0$  eV can be present in the case of  $CP$  violation as well.

Equation (44) permits us to express the cosine of the  $CP$ -violating phase  $(\alpha_3 - \alpha_2)$  in terms of measurable quantities:

$$\cos(\alpha_3 - \alpha_2) = \frac{|\langle m \rangle|^2 - \Delta m_{\odot}^2 \sin^4 \theta_{\odot} (1 - |U_{e3}|^2)^2 - \Delta m_{\text{atm}}^2 (|U_{e3}|^2)^2}{2\sqrt{\Delta m_{\odot}^2} \sqrt{\Delta m_{\text{atm}}^2} \sin^2 \theta_{\odot} |U_{e3}|^2 (1 - |U_{e3}|^2)}. \quad (60)$$

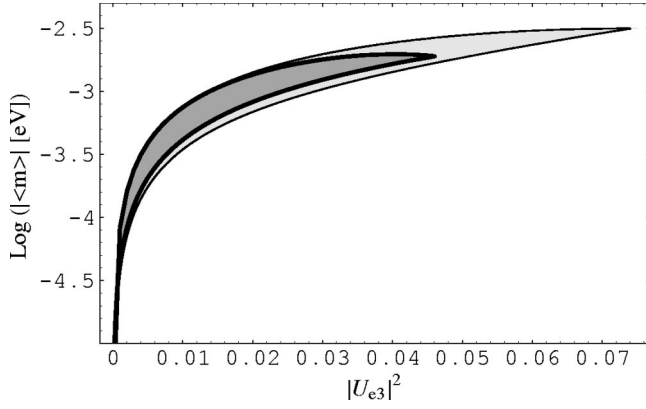


FIG. 4. The same as Fig. 2 but for  $\Delta m_{\odot}^2$  and  $\sin^2 \theta_{\odot}$  from the region of the SMA solution of the  $\nu_{\odot}$  problem [58] obtained at 90% C.L. (region within the thick solid lines) and at 99% C.L. (region within the thin solid lines). The results shown are derived assuming  $m_1 \ll 10^{-4}$  eV. For the range of values of  $|\langle m \rangle|$  in the figure, one has in this case  $|\langle m \rangle| \sim \sqrt{\Delta m_{\text{atm}}^2} |U_{e3}|^2$  and thus  $|\langle m \rangle|$  does not depend on the  $CP$ -violating phase ( $\alpha_3 - \alpha_2$ ).

Thus, if  $|\langle m \rangle|$  and  $|U_{e3}|^2$  are found to be nonzero and their values (together with the values of  $\Delta m_{\odot}^2$ ,  $\Delta m_{\text{atm}}^2$ , and  $\sin^2 \theta_{\odot}$ ) are determined experimentally with sufficient precision, one can get direct information about  $CP$  violation in the lepton sector, caused by Majorana  $CP$ -violating phases. In Fig. 5 we show the allowed range of  $\cos(\alpha_2 - \alpha_3)$  as a function of  $|\langle m \rangle|$  for different values of  $|U_{e3}|^2$ , using the best fit values for  $\Delta m_{\text{atm}}^2$ ,  $\Delta m_{\odot}^2$ , and  $\theta_{\odot}$  from [58].

Let us note that even if it is found that  $\alpha_3 - \alpha_2 = 0, \pm \pi$ , this will not necessarily mean that there is no  $CP$  violation due to the Majorana  $CP$ -violating phases in the lepton sector because the second of the two physical  $CP$ -violating phases is not constrained and can be a source of  $CP$  violation in other  $\Delta L = 2$  processes.

It follows from the analysis presented in this section that in the case of three-neutrino mixing and a hierarchical neutrino mass spectrum, the values of  $|\langle m \rangle|$  compatible with the neutrino oscillation-transition interpretation of the solar and atmospheric neutrino data and with the CHOOZ limit are smaller than  $5 \times 10^{-3}$  eV for the SMA and LOW-QVO so-

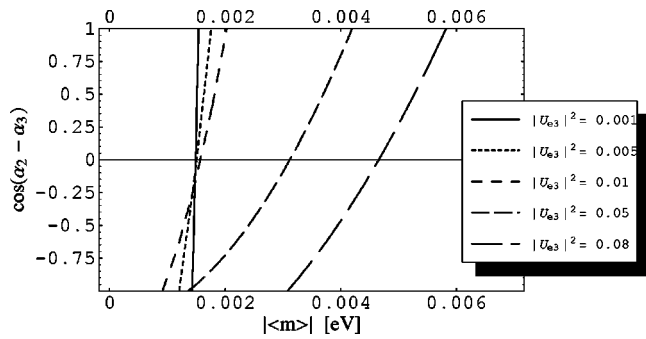


FIG. 5. The  $CP$ -violation factor  $\cos(\alpha_2 - \alpha_3)$ , Eq. (40) (hierarchical neutrino mass spectrum), as a function of  $|\langle m \rangle|$  for different values of  $|U_{e3}|^2$  and for the best fit values of the parameters  $\Delta m_{\odot}^2$ ,  $\sin^2 \theta_{\odot}$ , and  $\Delta m_{\text{atm}}^2$ , found in the analysis [58]. Values of  $\cos(\alpha_2 - \alpha_3) = 0, \pm 1$  correspond to  $CP$  invariance.

lutions of the solar neutrino problem. For the LMA solution one can have  $\max(|\langle m \rangle|) \cong (1-2) \times 10^{-2}$  eV. If the exchange of three relatively light Majorana neutrinos is the only mechanism generating the  $(\beta\beta)_{0\nu}$  decay, an observation of the latter with a lifetime corresponding to  $|\langle m \rangle| \cong 10^{-2}$  eV would practically rule out a hierarchical neutrino mass spectrum for the SMA and LOW-QVO solutions; an experimentally measured value of  $|\langle m \rangle| \cong 2 \times 10^{-2}$  eV would strongly disfavor the hierarchical neutrino mass spectrum for the LMA solution as well. In such a situation one would be led to conclude that at least two of the three massive Majorana neutrinos are quasidegenerate in mass.

## V. INVERTED MASS HIERARCHY SPECTRUM

The inverted mass hierarchy spectrum is characterized by the following relation between the neutrino masses  $m_j$ :

$$m_1 \ll m_2 \approx m_3. \quad (61)$$

The identification with the neutrino oscillation parameters probed in the solar and atmospheric neutrino experiments and in CHOOZ reads (see, e.g., [37,47,60])

$$\begin{aligned} \Delta m_{\odot}^2 &\equiv \Delta m_{32}^2, \\ \Delta m_{\text{atm}}^2 &\equiv \Delta m_{31}^2 \approx \Delta m_{21}^2, \\ |U_{e1}|^2 &= \sin^2 \theta < 0.09 \quad (\text{CHOOZ}), \\ |U_{e2}|^2 &= \cos^2 \theta_{\odot} (1 - |U_{e1}|^2), \\ |U_{e3}|^2 &= \sin^2 \theta_{\odot} (1 - |U_{e1}|^2). \end{aligned} \quad (62)$$

We also have

$$m_2 \approx m_3 \approx \sqrt{\Delta m_{\text{atm}}^2}. \quad (63)$$

The inverted mass hierarchy spectrum can also be defined by the inequalities

$$m_1 \ll (<) \sqrt{\Delta m_{32}^2} \ll \sqrt{\Delta m_{21}^2}. \quad (64)$$

The term  $m_1 |U_{e1}|^2$  in the expression for  $|\langle m \rangle|$ , Eq. (19), can be neglected, since  $m_1 \ll m_{2,3}$  and  $|U_{e1}|^2 \ll 1$ . This approximation would be valid as long as the sum of the two other terms in Eq. (19) exceeds  $\sim 5.0 \times 10^{-3}$  eV. Under the assumption that  $m_1 |U_{e1}|^2$  gives a negligible contribution to  $|\langle m \rangle|$  we have [37,46]

$$|\langle m \rangle| \approx ||U_{e2}|^2 m_2 + |U_{e3}|^2 m_3 e^{i(\alpha_3 - \alpha_2)}| \quad (65)$$

$$= m_{2,3} \sqrt{1 - 4|U_{e2}|^2 |U_{e3}|^2 \sin^2 \left( \frac{\alpha_3 - \alpha_2}{2} \right)} \quad (66)$$

$$= \sqrt{\Delta m_{\text{atm}}^2} (1 - |U_{e1}|^2) \sqrt{1 - \sin^2 2\theta_{\odot} \sin^2 \left( \frac{\alpha_3 - \alpha_2}{2} \right)}, \quad (67)$$

where we have used Eqs. (62) and (63). We see again that even though one of the three massive Majorana neutrinos

“decouples,” the value of  $|\langle m \rangle|$  depends on the Majorana  $CP$ -violating phase ( $\alpha_3 - \alpha_2$ ) [23]. In contrast, there cannot be  $CP$ -violation effects in the mixing of *only two* massive Dirac neutrinos.

It follows, e.g., from Eq. (67) that  $|\langle m \rangle|$  satisfies the inequalities [37,46]

$$\begin{aligned} \sqrt{\Delta m_{\text{atm}}^2}(1 - |U_{e1}|^2)|\cos 2\theta_{\odot}| &\leq |\langle m \rangle| \\ &\leq \sqrt{\Delta m_{\text{atm}}^2}(1 + |U_{e1}|^2). \end{aligned} \quad (68)$$

The upper and lower limits in Eq. (68) correspond respectively to the  $CP$ -conserving cases  $\phi_2 = \phi_3$  ( $\alpha_3 - \alpha_2 = 0$  or  $\alpha_{21} = \alpha_{31} = 0, \pm\pi$ ) and  $\phi_2 = -\phi_3$  ( $\alpha_3 - \alpha_2 = \pm\pi$  or  $\alpha_{21} = \alpha_{31} + \pi = 0, \pm\pi$ ).

If  $CP$  invariance holds in the leptonic sector, the parameters which determine  $|\langle m \rangle|$  are (i)  $\Delta m_{\text{atm}}^2$ , on the possible values of which there is a general agreement, (ii)  $(1 - |U_{e1}|^2) > 0.91$ , and (iii)  $|\cos 2\theta_{\odot}|$ , if  $\phi_2 = -\phi_3$ , whose allowed range varies with the analysis (see Table II). Consider the two cases of  $CP$  conservation.

*Case A.* If  $\nu_2$  and  $\nu_3$  have the same  $CP$  parities,  $\phi_2 = \phi_3$  ( $\alpha_{32} = 0$  or  $\alpha_{21} = \alpha_{31} = 0, \pm\pi$ ), the effective Majorana mass  $|\langle m \rangle|$  does not depend on  $|\cos 2\theta_{\odot}|$ :

$$|\langle m \rangle| = \sqrt{\Delta m_{\text{atm}}^2}(1 - |U_{e1}|^2). \quad (69)$$

Exploiting the 90% (99%) C.L. results of Ref. [58] we find that  $|\langle m \rangle|$  can take the values

$$3.7(3.3) \times 10^{-2} \text{ eV} \leq |\langle m \rangle| \leq 6.8(8.1) \times 10^{-2} \text{ eV}.$$

The “best fit” value is found to be

$$|\langle m \rangle|_{\text{BF}} = 5.6 \times 10^{-2} \text{ eV}.$$

For the results obtained in Refs. [55,64] we get

$$4.4(3.6) \times 10^{-2} \text{ eV} \leq |\langle m \rangle| \leq 8.1(8.9) \times 10^{-2} \text{ eV}.$$

All indicated values of  $|\langle m \rangle|$  can be probed in the next generation of  $(\beta\beta)_{0\nu}$ -decay experiments like GENIUS, EXO, etc.

*Case B.* For  $\nu_2$  and  $\nu_3$  having opposite  $CP$  parities,  $\phi_2 = -\phi_3$  ( $\alpha_{32} = \pm\pi$  or  $\alpha_{21} = \alpha_{31} + \pm\pi = 0, \pm\pi$ ), we have

$$|\langle m \rangle| = \sqrt{\Delta m_{\text{atm}}^2}(1 - |U_{e1}|^2)|\cos 2\theta_{\odot}|.$$

The ranges of values  $|\langle m \rangle|$  can have in this case are reported in Table III. The “best fit” value, according to the results in Ref. [58], is  $|\langle m \rangle|_{\text{BF}} = 2.1 \times 10^{-2} \text{ eV}$  (with the best fit  $\Delta m_{\odot}^2$  and  $\sin^2\theta_{\odot}$  lying in the LMA solution region). Note that for the SMA solution one has  $\cos 2\theta_{\odot} \simeq 1$  and  $|\langle m \rangle|$  has the same value in the two cases  $\phi_2 = -\phi_3$  and  $\phi_2 = \phi_3$ .

The results derived in the present section are illustrated and summarized in Figs. 6, 7, 8, and 9. In Figs. 6 and 7 we show the allowed regions of  $|\langle m \rangle|$  for the LMA and LOW-QVO solutions, respectively, as a function of  $\sqrt{\Delta m_{\text{atm}}^2}$ . It is interesting to note that there is a region, marked by dark-gray

TABLE III. Values  $|\langle m \rangle|$  compatible with the neutrino oscillation-transition interpretation of the solar and atmospheric neutrino data and with the CHOOZ limit in the case of neutrino mass spectrum with inverted hierarchy, Eq. (61),  $CP$  conservation, and  $\phi_2 = -\phi_3$  (see text for details).

Data from		$ \langle m \rangle $ [eV]
Refs. [7,55,64] (95% C.L.)	LMA	$7.3 \times 10^{-3} - 5.7 \times 10^{-2}$
	LOW-QVO	$0.9 \times 10^{-2} - 4.5 \times 10^{-2}$
Ref. [55,56,64] [90% (99%) C.L.]	LMA	$1.1 \times 10^{-2} (0.0) - 5.3 (5.9) \times 10^{-2}$
	SMA	$(3.6 \times 10^{-2} - 8.9 \times 10^{-2})$
Ref. [58] [90% (99%) C.L.]	LOW-QVO	$2.2 \times 10^{-3} (0.0) - 2.1 (3.7) \times 10^{-2}$
	LMA	$0(0) - 4.8 (5.8) \times 10^{-2}$
	SMA	$3.7 (3.3) \times 10^{-2} - 6.8 (8.1) \times 10^{-2}$
	LOW-QVO	$0(0) - 3.4 (5.4) \times 10^{-2}$

color, which can be spanned *only in the presence of CP violation*, i.e., this is a “just- $CP$ -violation” region. Thus, for the LMA and LOW-QVO solutions of the solar neutrino problem and neutrino mass spectrum of the type (61), an experimentally measured value of  $|\langle m \rangle|$  lying in the indicated region will signal the existence of  $CP$  violation in the leptonic sector, caused by Majorana  $CP$ -violating phases. A similar region is present and the above conclusion remains valid if we perform an analysis using the results of Refs. [56] and [7] for the LMA and LOW-QVO solutions, as Figs. 8 and 9 demonstrate.

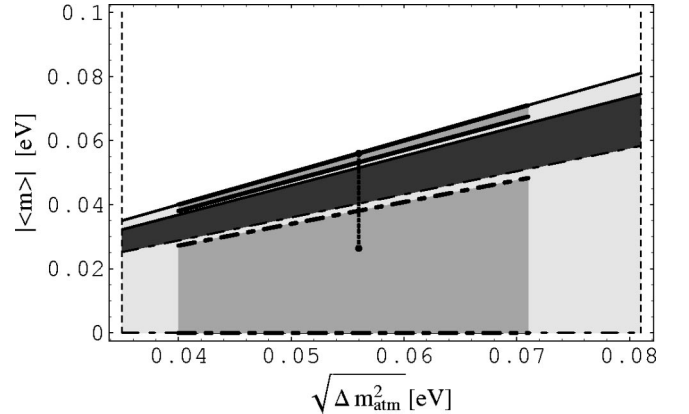


FIG. 6. The effective Majorana mass  $|\langle m \rangle|$  as a function of  $\sqrt{\Delta m_{\text{atm}}^2}$  for the neutrino mass spectrum of the inverted hierarchy type, Eq. (61). The allowed regions (in gray) correspond to the LMA solution of Ref. [58]. In the case of  $CP$  invariance and for the 90% (99%) C.L. results for the solution region,  $|\langle m \rangle|$  can have values (i) for  $\phi_2 = \phi_3$ , in the medium-gray (light-gray and medium-gray) upper region, limited by the doubly thick (thick and doubly thick) solid lines, and (ii) for  $\phi_2 = -\phi_3$ , in the medium-gray (light-gray and medium-gray) region, limited by the doubly thick (thick and doubly thick) dash-dotted lines. If  $CP$  is not conserved,  $|\langle m \rangle|$  can lie in any of the regions marked by different gray scales. The dark-gray region corresponds to “just- $CP$ -violation:”  $|\langle m \rangle|$  can have a value in this region *only if the CP parity is not conserved*. The values of  $|\langle m \rangle|$  corresponding to the best fit values of the input parameters, found in [58], are denoted by dots in the  $CP$ -conserving cases and by a dotted line in the  $CP$ -violating one.

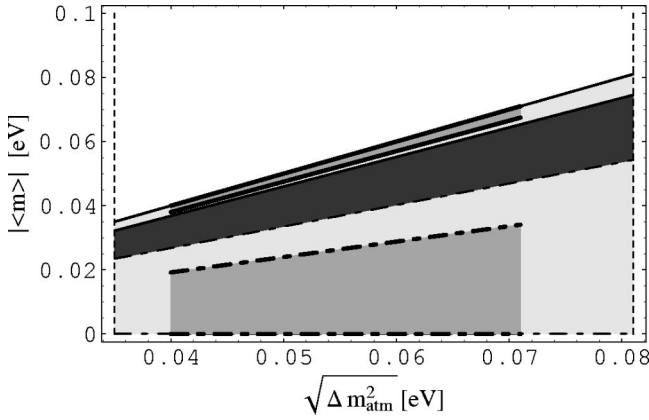


FIG. 7. The same as in Fig. 6 for the 90% (99%) C.L. LOW-QVO solution of Ref. [58]. The medium-gray (light-gray and medium-gray) region, bounded by the thick (thick and doubly thick) solid lines, and medium-gray (light-gray and medium-gray) lower region, bounded by the thick (thin) dash-dotted lines, correspond to the two cases of  $CP$  invariance,  $\phi_2 = \phi_3$  and  $\phi_2 = -\phi_3$ , respectively. If  $CP$  is not conserved,  $|\langle m \rangle|$  can lie in any of the regions marked by different gray scales. The “just- $CP$ -violation” region is shown in dark-gray color:  $|\langle m \rangle|$  can have a value in this region *only if the  $CP$  symmetry is violated*.

It would be practically impossible to obtain information on  $CP$  violation in the leptonic sector due to the Majorana  $CP$ -violating phases by measuring  $|\langle m \rangle|$  if the SMA solution of the solar neutrino problem turns out to be the valid one.

For all solutions of the solar neutrino problem we have  $|\langle m \rangle| \lesssim (0.08-0.09)$  eV for the inverted mass hierarchy neutrino mass spectrum. In large allowed regions of the corre-

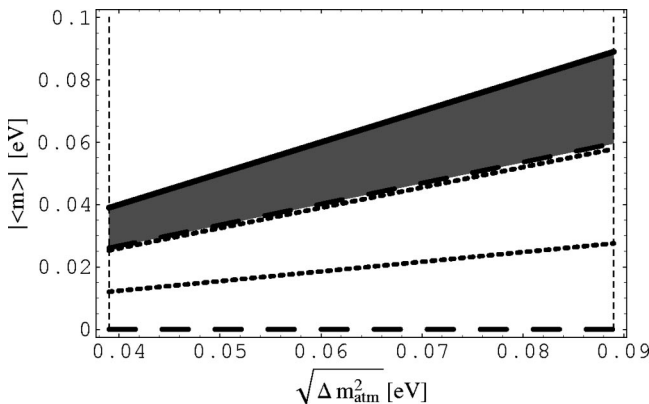


FIG. 8.  $|\langle m \rangle|$  as a function of  $\sqrt{\Delta m_{\text{atm}}^2}$  for the inverted mass hierarchy spectrum and LMA solution of the solar neutrino problem. The figure is obtained using the results of Ref. [7] (region between the thick solid line and the lower dotted line) and of Ref. [56] (at 99% C.L., region between the thick solid line and the lower long-dashed line). If  $CP$  invariance does not hold,  $|\langle m \rangle|$  spans all the allowed regions indicated (in brackets) above. The values of  $|\langle m \rangle|$  in the two  $CP$ -conserving cases lie (i) on the doubly thick solid line if  $\phi_2 = \phi_3$ , and (ii) for  $\phi_2 = -\phi_3$  between the two dotted lines (dashed lines) for the LMA solution in Ref. [7] (Ref. [56]). The common “just- $CP$ -violation” region for both analyses is marked in dark gray: *a value of  $|\langle m \rangle|$  in this region would signal  $CP$  violation*.

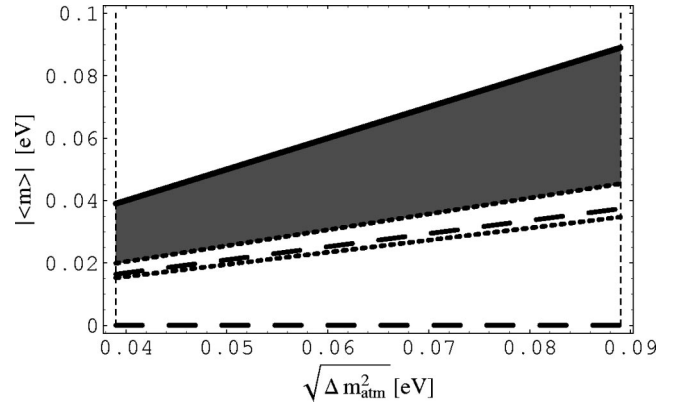


FIG. 9. The same as in Fig. 8 for the LOW-QVO solution found in Refs. [7] and [56] (at 99% C.L.). The “just- $CP$ -violation” region, in particular, is marked by dark-gray color.

sponding parameter space we have  $|\langle m \rangle| \gtrsim (0.01-0.02)$  eV, which can be tested in the future  $(\beta\beta)_{0\nu}$ -decay experiments like GENIUS, EXO, etc.

As the dependence of  $|\langle m \rangle|$  on  $\cos 2\theta_{\odot}$  is rather strong, in Fig. 10 we plot  $|\langle m \rangle|$  versus  $\cos 2\theta_{\odot}$ . The region of values of  $|\langle m \rangle|$ , corresponding to the “just  $CP$  violation,” is marked by the dark-gray color. The uncertainty in the allowed ranges of  $|\langle m \rangle|$  for the two different values of the relative  $CP$  parity of  $\nu_2$  and  $\nu_3$  is due mainly to the uncertainty in the value of  $\Delta m_{\text{atm}}^2$ . If the value of  $\Delta m_{\text{atm}}^2$  is better constrained and  $|\langle m \rangle|$  is found to lie in the regions corresponding to the LMA or LOW-QVO solution, it would be possible to establish in the case of the mass spectrum (61) if

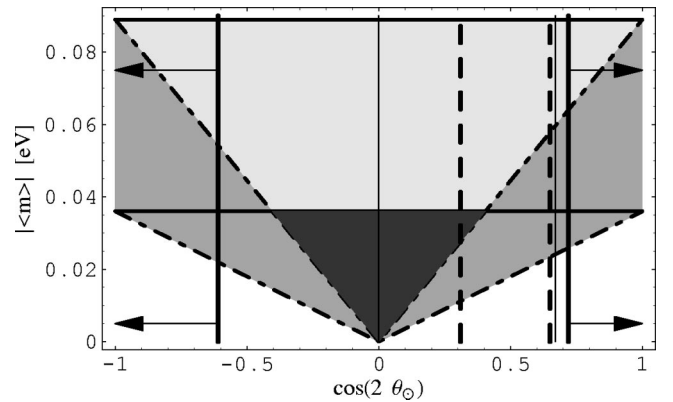


FIG. 10. The dependence of  $|\langle m \rangle|$  on  $\cos 2\theta_{\odot}$  for the neutrino mass spectrum with inverted hierarchy, Eq. (61), and the LMA solution of the solar neutrino problem. The region between the two thick horizontal solid lines (in light-gray and medium-gray colors) and the two triangular regions between the thick dash-dotted lines (in medium-gray color), correspond to the two  $CP$ -conserving cases,  $\phi_2 = \phi_3$  and  $\phi_2 = -\phi_3$ , respectively. The “just- $CP$ -violation” region is denoted by dark-gray color. The regions between each of the three pairs of vertical lines of a given type, solid, doubly thick solid, and doubly thick dashed lines, correspond to the intervals of values of  $\cos 2\theta_{\odot}$  for the LMA solution derived (at 99% C.L.) in Ref. [7] (region between the two doubly thick dashed lines), Ref. [56] (region between the solid lines), and Ref. [58].

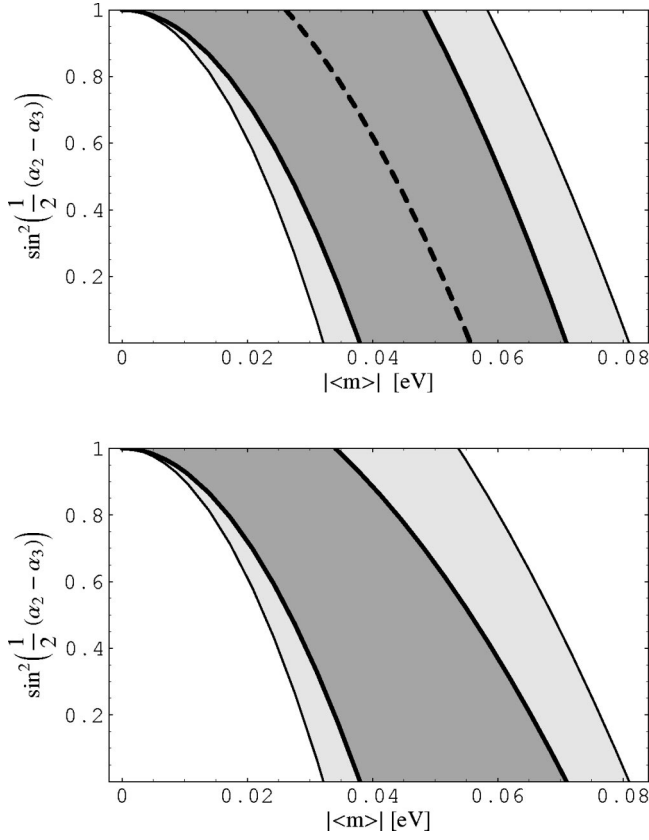


FIG. 11. The  $CP$ -violation factor  $\sin^2(\alpha_2 - \alpha_3)/2$  as a function of  $|\langle m \rangle|$  in the case of an inverted mass hierarchy spectrum, Eq. (61), and the LMA (upper panel) and LOW-QVO (lower panel) solutions of Ref. [58], obtained at 90% C.L. (medium-gray region with thick contours) and 99% C.L. (light-gray and medium-gray regions delimited by ordinary solid lines). The values of  $|\langle m \rangle|$ , corresponding to the best fit values of the input parameters, found in [58], are indicated by the dashed line. A value of  $\sin^2(\alpha_2 - \alpha_3)/2 \neq 0,1$  would signal  $CP$  violation.

$CP$  is violated and to get information on the value of one of the two  $CP$ -violating phases ( $\alpha_3 - \alpha_2$ ).

Equation (67) permits us to relate the value of  $\sin^2(\alpha_3 - \alpha_2)/2$  to the experimentally measured quantities  $|\langle m \rangle|$ ,  $\Delta m_{\text{atm}}^2$ , and  $\sin^2 2\theta_\odot$ :

$$\sin^2 \frac{\alpha_3 - \alpha_2}{2} = \left( 1 - \frac{|\langle m \rangle|^2}{\Delta m_{\text{atm}}^2 (1 - |U_{e1}|^2)^2} \right) \frac{1}{\sin^2 2\theta_\odot}. \quad (70)$$

A more precise determination of  $\Delta m_{\text{atm}}^2$  and  $\theta_\odot$  and a sufficiently accurate measurement of  $|\langle m \rangle|$  could allow us to get information about the value of  $(\alpha_3 - \alpha_2)$ , provided the neutrino mass spectrum is of the inverted hierarchy type (61). This is illustrated in Fig. 11 for the cases of the LMA and LOW-QVO solutions. We would like to point out also that, as in the case of a hierarchical neutrino mass spectrum, even if one finds using the  $(\beta\beta)_{0\nu}$ -decay data that the phase  $(\alpha_3 - \alpha_2) = 0, \pm\pi$  and does not violate  $CP$  invariance, the second phase  $(\alpha_2 - \alpha_1) \equiv \alpha_{21}$  is not constrained and can be a source of  $CP$  violation in other  $\Delta L = 2$  processes.

The results derived in the present section show that in the case of massive Majorana neutrinos and the neutrino mass spectrum of the inverted hierarchy type, Eq. (61), the description of the solar and atmospheric neutrino data in terms of neutrino oscillations and transitions and the CHOOZ limit imply an upper limit on the effective Majorana mass parameter:  $|\langle m \rangle| \lesssim (8-9) \times 10^{-2}$  eV. A measured value of  $|\langle m \rangle| \gtrsim (2-3) \times 10^{-1}$  eV would strongly disfavor, under the general assumptions of the present study [three-neutrino mixing,  $(\beta\beta)_{0\nu}$  decay generated only by the charged  $(V-A)$  current weak interaction via the exchange of the three Majorana neutrinos], the possibility of inverted neutrino mass hierarchy.

## VI. CASE OF THREE QUASIDEGENERATE NEUTRINOS

The neutrinos  $\nu_{1,2,3}$  are quasidegenerate in mass if

$$m_1 \simeq m_2 \simeq m_3 \equiv m \quad (71)$$

and

$$m \gtrsim \sqrt{\Delta m_{\text{atm}}^2}. \quad (72)$$

When Eq. (71) holds but  $m \sim O(\sqrt{\Delta m_{\text{atm}}^2})$ , we have a partial hierarchy or partial inverted hierarchy between the neutrino masses. These two possibilities will be considered in the next section. The possible implications of quasidegenerate neutrino mass spectrum for  $|\langle m \rangle|$  were discussed recently also in [53], but from a somewhat different point of view.

As for the hierarchical neutrino mass spectrum we have

$$\Delta m_\odot^2 \equiv \Delta m_{21}^2, \quad \Delta m_{\text{atm}}^2 \equiv \Delta m_{32}^2,$$

$$|U_{e1}|^2 = \cos^2 \theta_\odot (1 - |U_{e3}|^2),$$

$$|U_{e2}|^2 = \sin^2 \theta_\odot (1 - |U_{e3}|^2),$$

$$|U_{e3}|^2 = \sin^2 \theta < 0.09 \quad (\text{CHOOZ}). \quad (73)$$

The parameters  $\Delta m_{\text{atm}}^2$ ,  $\Delta m_\odot^2$ , and  $\theta_\odot$  take values in the regions quoted in Sec. II. Equation (73) allows to express Eqs. (71) and (72) in the compact form

$$\sqrt{\Delta m_{21}^2} \ll (<) \sqrt{\Delta m_{32}^2} \ll m_1. \quad (74)$$

As can be shown (see, e.g., [48,60]), the mass scale  $m$  effectively coincides with the electron (anti)neutrino mass  $m_{\nu_e}$  measured in the  ${}^3\text{H}$   $\beta$ -decay experiments:

$$m = m_{\nu_e}. \quad (75)$$

Thus, the experimental upper bounds in Eq. (13) lead to  $m < 2.5$  eV.

The quasidegenerate neutrino mass spectrum under discussion is actually realized for values of the neutrino mass  $m$ , which is measured in the  ${}^3\text{H}$   $\beta$ -decay experiments,  $m = m_{\nu_e} \gtrsim (0.2-0.3)$  eV (see Sec. VII for a more detailed discussion). Recently, the Karlsruhe, Mainz, and Troitzk Collaborations proposed a new  ${}^3\text{H}$   $\beta$ -decay experiment KATRIN [69], which is planned to have a record sensitivity of 0.35 eV to

TABLE IV. Values of  $|\langle m \rangle|/m$  for the quasidegenerate neutrino mass spectrum, Eq. (71),  $CP$  conservation, and  $\phi_1 = -\phi_2 = \pm\phi_3$  (see text for details).

Data from		$ \langle m \rangle /m$	
		$\phi_1 = -\phi_2 = \phi_3$	$\phi_1 = -\phi_2 = -\phi_3$
Ref. [7] (95% C.L.)	LMA	0.21–0.68	0.10–0.65
	LOW-QVO	0.30–0.58	0.18–0.54
Ref. [56] [90% (99%) C.L.]	LMA	0.25 (0)–0.68 (0.70)	0.12 (0)–0.65 (0.67)
	SMA	(1.0)	(0.8–1.0)
Ref. [58] [90% (99%) C.L.]	LOW-QVO	0.05 (0)–0.33 (0.49)	0 (0)–0.26 (0.42)
	LMA	0 (0)–0.70 (0.74)	0 (0)–0.68 (0.72)
	SMA	1.0 (1.0)	0.9 (0.8)–1.0 (1.0)
	LOW-QVO	0 (0)–0.50 (0.69)	0 (0)–0.48 (0.67)

the neutrino mass  $m_{\nu_e}$ . Clearly, the realization of this project could be crucial for the test of the possibility of three quasidegenerate neutrinos.

It follows from Eqs. (71), (72) and Eq. (19) that  $|\langle m \rangle|$  can be approximated by<sup>7</sup>

$$|\langle m \rangle| \approx m |\cos^2 \theta_\odot (1 - |U_{e3}|^2) e^{i\alpha_1} + \sin^2 \theta_\odot (1 - |U_{e3}|^2) e^{i\alpha_2} + |U_{e3}|^2 e^{i\alpha_3}|. \quad (76)$$

If  $CP$  is conserved, we have the following possibilities, depending on the relative  $CP$  parities of the neutrinos  $\nu_j$ .

*Case A.* For  $\phi_1 = \phi_2 = \pm\phi_3$  (i.e.,  $\alpha_{21} = 0$ ,  $\alpha_{31} = 0, \pm\pi$ ), we get a very simple expression for  $|\langle m \rangle|$ :

$$|\langle m \rangle| \approx m (1 - |U_{e3}|^2 \pm |U_{e3}|^2); \quad (77)$$

i.e.,  $|\langle m \rangle|$  does not depend on  $\Delta m_\odot^2$ ,  $\theta_\odot$ , and  $\Delta m_{\text{atm}}^2$ . Note that if  $\phi_1 = \phi_2 = \phi_3$ ,  $|\langle m \rangle| = m$ . Using the CHOOZ limit [64] on  $|U_{e3}|^2$  one finds the range of allowed values of  $|\langle m \rangle|$ :

$$0.8m \leq |\langle m \rangle| \leq 1.0m. \quad (78)$$

The above result and the bound on  $|\langle m \rangle|$  obtained in the Heidelberg-Moscow experiment [29], Eq. (4), imply

$$m < (0.4 - 1.2) \text{ eV}, \quad (79)$$

which is compatible with the  ${}^3\text{H}$  beta-decay limit on  $m$ .

*Case B.* If  $\phi_1 = -\phi_2 = \pm\phi_3$  (i.e.,  $\alpha_{21} = \pm\pi$ ,  $\alpha_{31} = 0, \pm\pi$ ),  $|\langle m \rangle|$  is given by

$$|\langle m \rangle| \approx m |\cos 2\theta_\odot (1 - |U_{e3}|^2) \pm |U_{e3}|^2|. \quad (80)$$

Now  $|\langle m \rangle|$  depends on  $\cos 2\theta_\odot$  and thus varies with solution of the solar neutrino problem. For the LMA and LOW-QVO solutions, the expression for  $|\langle m \rangle|$  in the case of  $\cos 2\theta_\odot > 0$  and  $\phi_1 = -\phi_2 = \phi_3$  coincides with that for  $\cos 2\theta_\odot < 0$  and  $\phi_1 = -\phi_2 = -\phi_3$ . The allowed intervals of values of

$|\langle m \rangle|/m$  for the three solutions of the solar neutrino problem derived in [7,56,58] are reported in Table IV.

Several remarks are in order.

(1) In the case of the LMA solution, the 99% C.L. results of the analysis in Refs. [58,56] do not exclude the possibility of a cancellation between the different contributions in  $|\langle m \rangle|$ , so that

$$0 \leq |\langle m \rangle| \leq 0.7m.$$

The results of Ref. [7] for the same solution do not allow a complete cancellation to occur and one has

$$0.2 \times 10^{-2} m \leq |\langle m \rangle| \leq 0.7m.$$

(2) The results of all three analyses for the SMA solution agree. The case under discussion cannot be distinguished from the  $\phi_1 = \phi_2 = \pm\phi_3$  one since  $\cos 2\theta_\odot \approx 1$ .

(3) In the LOW-QVO solution case, the results of the analyses [56,58] do not exclude the possibility of cancellations between the different contributions in  $|\langle m \rangle|$ , as well as of having  $\cos 2\theta_\odot < 0$ , so that

$$0 \leq |\langle m \rangle| \leq (0.5 - 0.7)m.$$

In contrast, according to the results of the analysis [7],  $\cos 2\theta_\odot > 0$  and one finds a relatively large lower bound on  $|\langle m \rangle|$ .

The regions of allowed values of  $|\langle m \rangle|$ , corresponding to the LMA and the LOW-QVO solutions of Ref. [58], are shown as a function of  $m$  in Figs. 12 and 13, respectively. One can have  $|\langle m \rangle| \geq 0.1 \text{ eV}$  for values of  $m \geq 0.1 \text{ eV}$ . Taking into account the  ${}^3\text{H}$   $\beta$ -decay upper bound  $m < 2.5 \text{ eV}$ , we find that  $\max(|\langle m \rangle|) \approx 1.7 \text{ eV}$ . This implies that  $|\langle m \rangle|$  can have the maximal value allowed by the limit (4):  $\max(|\langle m \rangle|) < (0.35 - 1.05) \text{ eV}$ .

If  $CP$  parity is not conserved, one has to take into account the two relevant  $CP$ -violating phases  $\alpha_{21}$  and  $\alpha_{31}$  in the expression for  $|\langle m \rangle|$ . The effective mass  $|\langle m \rangle|$  can be computed using a graphical method [50,52]. Each of the three contributions to  $|\langle m \rangle|$  can be represented by a vector,  $\mathbf{n}_j$ ,  $j = 1, 2, 3$ , in the complex plane, as sketched in Fig. 1:  $\mathbf{n}_1 = m_1 |U_{e1}|^2 (1, 0)$ ,  $\mathbf{n}_2 = m_2 |U_{e2}|^2 (\cos \alpha_{21}, \sin \alpha_{21})$ ,  $\mathbf{n}_3 = m_2 |U_{e3}|^2 (\cos \alpha_{31}, \sin \alpha_{31})$ . The two phases  $\alpha_{21}$  and  $\alpha_{31}$

<sup>7</sup>Under the assumption that the terms  $\sim |U_{e3}|^2$  give a negligible contribution in  $|\langle m \rangle|$ , this case was considered briefly recently in [78].

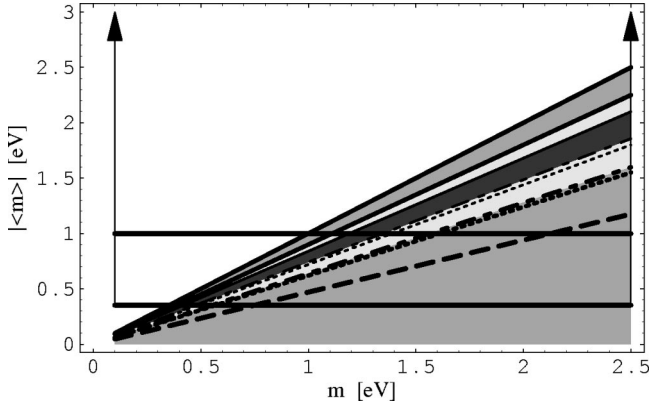


FIG. 12.  $|\langle m \rangle|$  as a function of the neutrino mass  $m$  for the quasidegenerate neutrino mass spectrum, Eqs. (71),(72), and the LMA solution of the  $\nu_\odot$  problem of Ref. [58] at 90% C.L. (99% C.L.). The regions allowed in the cases of  $CP$  conservation are marked by (i)  $\phi_1 = \phi_2 = \phi_3$ , the doubly thick solid (nonhorizontal) line  $|\langle m \rangle| = m$ , (ii)  $\phi_1 = \phi_2 = -\phi_3$ , medium-gray color triangular region between the two doubly thick solid lines (light-gray and medium-gray color triangular regions between the doubly thick and thick solid lines (iii)  $\phi_1 = -\phi_2 = \pm\phi_3$  (two cases), medium-gray color triangular regions between the doubly thick dashed-dotted line and the horizontal axes (light-gray and medium-gray regions between the thin dashed-dotted line and the horizontal axes and between the thin dotted line and the horizontal axes). The “just- $CP$ -violation” region is denoted by dark-gray color. The doubly thick solid line corresponding to  $|\langle m \rangle| = m$  and the doubly thick long dashed line indicate the “best fit lines” of values of  $|\langle m \rangle|$  for the (i), (ii), and the (iii) cases, respectively. The two horizontal (doubly thick) lines show the upper limits [29], quoted in Eq. (3).

can take values from 0 to  $2\pi$  and the effective Majorana mass  $|\langle m \rangle|$  is given by the modulus of the sum of the three vectors:  $|\langle m \rangle| = |\mathbf{n}_1 + \mathbf{n}_2 + \mathbf{n}_3|$ .

In order to have a complete cancellation between the three terms in  $|\langle m \rangle|$ , Eq. (76), the following condition has to be satisfied (see also [52]):

$$|m_1 U_{e1}^2| < |m_2 U_{e2}^2| + |m_3 U_{e3}^2|. \quad (81)$$

The relation (71) between the masses  $m_j$ , Eq. (72) and the identification (73), imply that this inequality reduces to a condition on the angle  $\theta_\odot$  and on  $|U_{e3}|^2$ :

$$\cos^2 \theta_\odot < \frac{1}{2(1 - |U_{e3}|^2)}. \quad (82)$$

Using the results of the different data analyses which are summarized in Sec. II and in Tables I and II, we can conclude the following.

(1) A complete cancellation between the three terms in  $|\langle m \rangle|$ , Eq. (76), is impossible for the SMA solution of the solar neutrino problem.

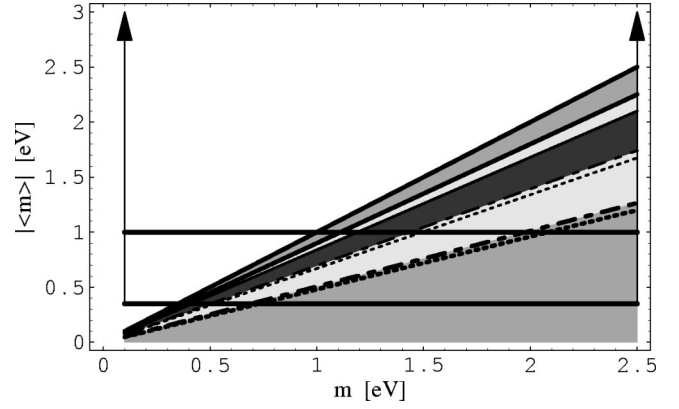


FIG. 13. The same as in Fig. 12 for the LOW-QVO solution of the  $\nu_\odot$  problem [58]. If  $CP$  is conserved and at 90% C.L. (99% C.L.) [58],  $|\langle m \rangle|$  should lie in the two medium-gray (the two light-gray and medium-gray) triangular regions: (i) for  $\phi_1 = \phi_2 = \phi_3$ , on the line  $|\langle m \rangle| = m$ , (ii) for  $\phi_1 = \phi_2 = -\phi_3$ , in the upper medium-gray (light-gray and medium-gray) triangular region, (iii) if  $\phi_1 = -\phi_2 = \pm\phi_3$ , in the lower medium-gray (light-gray and medium-gray) triangular region with dash-dotted ( $\phi_1 = +\phi_3$ ) and dotted ( $\phi_1 = -\phi_3$ ) contours. The “just- $CP$ -violation” region is denoted by dark-gray color.

(2) The results on the possible values of  $\theta_\odot$  in [58] and [56] (Table II) show that there can be a complete cancellation both in the case of the LMA and LOW-QVO solutions.

(3) According to the analysis of Ref. [7], there can be a cancellation in the LOW-QVO case but not in the LMA one.

The lower and upper limits on  $|\langle m \rangle|$  can be found taking, respectively,  $\alpha_{21} = \alpha_{31} = \pm\pi$  (e.g.,  $\phi_1 = -\phi_2 = -\phi_3$ ) and  $\alpha_{21} = \alpha_{31} = 0$  (e.g.,  $\phi_1 = \phi_2 = \phi_3$ ). Recalling the limits already found in the  $CP$ -conserving cases, the bounds holding in the  $CP$ -violating one are reported in Table V.

We see that in the case of  $CP$  violation we can have  $|\langle m \rangle| \geq 0.1$  eV as well. The upper bound on  $m$  following from the  $^3\text{H}$   $\beta$ -decay data implies  $|\langle m \rangle| < 2.5$  eV, while the results (4) of the Heidelberg-Moscow  $(\beta\beta)_{0\nu}$ -decay experiment (including a factor of 3 uncertainty in the value of the relevant nuclear matrix element) limit further the maximal value of  $|\langle m \rangle|$  to  $\max(|\langle m \rangle|) < (0.35 - 1.05)$  eV. Let us remind the reader that, as our results in Secs. IV and V showed, one has  $\max(|\langle m \rangle|) \leq 0.02$  eV if the neutrino mass spectrum is hierarchical, Eq. (40), while in the case of inverted mass hierarchy, Eq. (61),  $\max(|\langle m \rangle|) \leq (0.08 - 0.09)$  eV. Thus, observation of  $(\beta\beta)_{0\nu}$  decay with a rate which corresponds to  $|\langle m \rangle| \geq (0.20 - 0.30)$  eV would be very strong experimental evidence in favor of the quasidegenerate neutrino mass spectrum: this would practically rule out the neutrino mass spectrum of the hierarchical type and would strongly disfavor (if not rule out) that of the inverse mass hierarchy type. The above conclusion would be valid, of course, only if the  $(\beta\beta)_{0\nu}$  decay is generated by the charged current weak interaction with left-handed currents and three-neutrino mixing, via the exchange of three massive Majorana neutrinos.

The improvement of the sensitivity of the  $^3\text{H}$   $\beta$ -decay experiments would allow one to test further the pattern of



TABLE V. Values of  $|\langle m \rangle|/m$ , corresponding to the different solutions of the solar neutrino problem, neutrino oscillation interpretation of the atmospheric neutrino data and the CHOOZ limit, in the case of a quasidegenerate neutrino mass spectrum, Eq. (71), and  $CP$  nonconservation (see text for details).

Data from		$ \langle m \rangle /m$
Ref. [7]	LMA	0.10–1.0
(95% C.L.)	LOW-QVO	0.18–1.0
Ref. [56]	LMA	0.12 (0)–1.0 (1.0)
[90% (99%) C.L.]	SMA	(0.8–1.0)
	LOW-QVO	0 (0)–1.0 (1.0)
Ref. [58]	LMA	0 (0)–1.0 (1.0)
[90% (99%) C.L.]	SMA	0.9 (0.8)–1.0 (1.0)
	LOW-QVO	0 (0)–1.0 (1.0)

neutrino masses (71),(72). The  $(\beta\beta)_{0\nu}$ -decay experiments could distinguish between the different  $CP$ -parity configurations of the massive neutrinos  $\nu_j$  and furthermore either establish the existence of  $CP$  violation in the leptonic sector or put an upper bound on its possible magnitude. This is illustrated in Figs. 14 and 15 where we show  $|\langle m \rangle|/m$  as a function of  $\cos 2\theta_\odot$ . The dark-gray region is the “just- $CP$ -violation” region which can be spanned by the values of  $|\langle m \rangle|/m$  only if the  $CP$  symmetry is violated.

If  $\theta_\odot$ ,  $|U_{e3}|^2$ ,  $m$ , and  $|\langle m \rangle|$  are known with a sufficient accuracy, it would be possible to tightly constrain the allowed values of the two  $CP$ -violating Majorana phases  $\alpha_{21}$  and  $\alpha_{31}$  as they must satisfy the relation

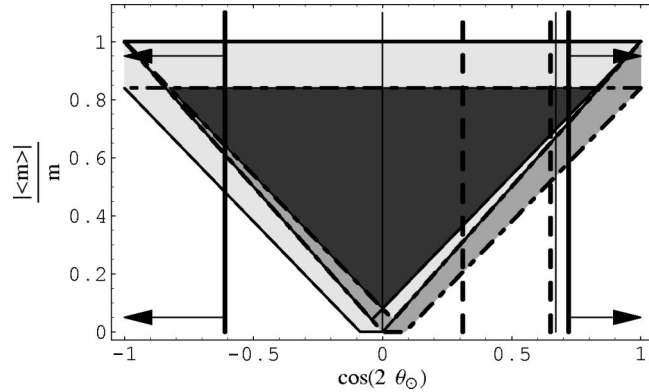


FIG. 14. The dependence of  $|\langle m \rangle|/m$  on  $\cos 2\theta_\odot$  for the quasidegenerate neutrino mass spectrum, Eqs. (71),(72), and the LMA solution of the  $\nu_\odot$  problem. If  $CP$  invariance holds, the values of  $|\langle m \rangle|/m$  lie: (i) for  $\phi_1 = \phi_2 = \phi_3$ , on the line  $|\langle m \rangle|/m = 1$ , (ii) for  $\phi_1 = \phi_2 = -\phi_3$ , in the region between the thick horizontal solid and dash-dotted lines (in light-gray and medium-gray colors), (iii) for  $\phi_1 = -\phi_2 = +\phi_3$ , in the light gray polygon with solid-line contours and iv) for  $\phi_1 = -\phi_2 = -\phi_3$ , in the medium-gray polygon with the dash-dotted-line contours. The “just- $CP$ -violation” region is denoted by dark-gray color. The values of  $\cos 2\theta_\odot$  between the doubly thick solid, the normal solid, and the doubly thick dashed lines correspond to the 99%, 99%, and 95% C.L. LMA solution regions in Refs. [58], [56], and [7], respectively.

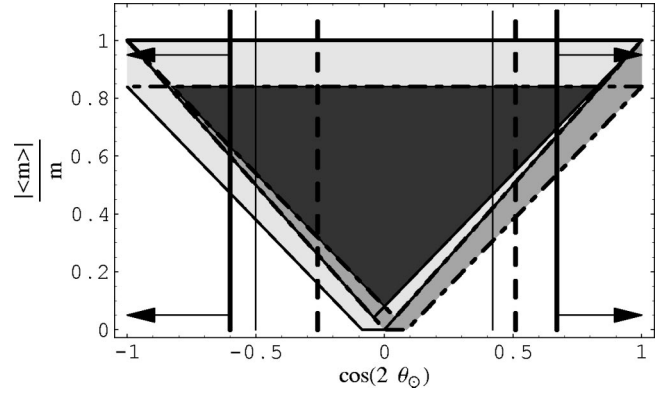


FIG. 15. The same as in Fig. 14 for the LOW-QVO solution of the solar neutrino problem. The “just- $CP$ -violating” region, in particular, is denoted by dark-gray color.

$$\begin{aligned}
 & \frac{|\langle m \rangle|^2}{m^2} - (\cos^4 \theta_\odot (1 - |U_{e3}|^2)^2 \\
 & + \sin^4 \theta_\odot (1 - |U_{e3}|^2)^2 + |U_{e3}|^4) \\
 & = 2 \cos^2 \theta_\odot |U_{e3}|^2 (1 - |U_{e3}|^2) \cos \alpha_{31} \\
 & + 2 \sin^2 \theta_\odot \cos^2 \theta_\odot (1 - |U_{e3}|^2)^2 \cos \alpha_{21} \\
 & + 2 \sin^2 \theta_\odot |U_{e3}|^2 (1 - |U_{e3}|^2) \cos(\alpha_{21} - \alpha_{31}).
 \end{aligned} \tag{83}$$

In Fig. 16 we exhibit the allowed values of  $\cos \alpha_{21}$  and  $\cos \alpha_{31}$  for a given value of  $|\langle m \rangle|/m$ : for the parameters entering into the expression (83) we use their best fit values from Ref. [58] (which lie in the LMA solution region, etc.),  $|U_{e3}|^2 = 0.005$  and  $|U_{e3}|^2 = 0.08$  and we allow  $|\langle m \rangle|$  to vary, respectively, in the intervals  $|\langle m \rangle| = 0.40m - 0.70m$  and  $|\langle m \rangle| = 0.20m - 0.50m$ .

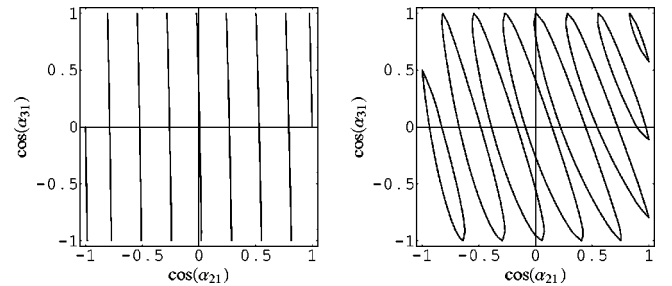


FIG. 16. The interdependence of the two  $CP$ -violating phases  $\alpha_{21}$  and  $\alpha_{31}$  for a given value of the ratio  $|\langle m \rangle|/m$  in the case of a quasidegenerate neutrino mass spectrum. The figures are obtained for  $|\langle m \rangle|/m = \sqrt{0.2+0.1n}$  eV with  $n=0,1,\dots,8$  (with increasing  $|\langle m \rangle|$  from left to right) and the best fit values of the solar and atmospheric neutrino oscillation parameters from [58], quoted in Sec. II (left-hand plot), and for  $|\langle m \rangle|/m = \sqrt{0.24+0.10n}$  eV with  $n=0,1,\dots,7$  (with increasing  $|\langle m \rangle|$  from left to right),  $|U_{e3}|^2 = 0.08$ , and the best fit values of the other solar and atmospheric neutrino oscillation parameters [58] (right-hand plot). The values of  $\cos \alpha_{21,31} = 0, \pm 1$ , correspond to  $CP$  invariance.

## VII. PARTIAL MASS HIERARCHY AND PARTIAL INVERTED MASS HIERARCHY CASES

The partial mass hierarchy and the partial inverted mass hierarchy spectra are characterized, respectively, by the following relations between the three neutrino masses:

$$m_1 \approx m_2 < m_3 \quad \text{or} \quad \Delta m_{21}^2 = \Delta m_{\odot}^2 \ll \Delta m_{32}^2 = \Delta m_{\text{atm}}^2 \sim O(m_1^2) \quad (84)$$

and

$$m_1 < m_2 \approx m_3 \quad \text{or} \quad \Delta m_{32}^2 = \Delta m_{\odot}^2 \ll \Delta m_{21}^2 = \Delta m_{\text{atm}}^2 \sim O(m_1^2). \quad (85)$$

The pattern (84) [(85)] interpolates between the hierarchical [inverted mass hierarchy] neutrino mass spectrum and the quasidegenerate one. The two intermediate types of neutrino mass spectrum Eqs. (84) and (85), were discussed also in [52]. We will consider in the subsequent analysis values of  $m_1$  from the interval  $0.02 \text{ eV} \leq m_1 \leq 0.2 \text{ eV}$ . These values of  $m_1$  are determined by the values of  $\Delta m_{\text{atm}}^2$ , obtained in the analyses of the atmospheric neutrino data, by requiring that  $1/5 \Delta m_{\text{atm}}^2|_{\text{MIN}} \leq m_1^2 \leq 5 \Delta m_{\text{atm}}^2|_{\text{MAX}}$ . For  $m_1 > 0.2 \text{ eV}$  one recovers the quasidegenerate neutrino mass spectrum. If  $m_1 \ll 0.02 \text{ eV}$ , we get the hierarchical or the inverted mass hierarchy spectrum. We will consider values of  $m_1$  not smaller than  $0.02 \text{ eV}$  also because for  $m_1 \ll 0.02 \text{ eV}$  the contributions of the term  $\sim m_1$  in  $|\langle m \rangle|$  amounts to a relatively small correction.

### A. Spectrum with partial mass hierarchy

Using Eqs. (19) and (84) and neglecting corrections  $\sim \Delta m_{\odot}^2/m_1^2$ , one can express the effective Majorana mass parameter  $|\langle m \rangle|$  in the form

$$|\langle m \rangle| = m_1 \left| \cos^2 \theta_{\odot} (1 - |U_{e3}|^2) e^{i\alpha_1} + \sin^2 \theta_{\odot} (1 - |U_{e3}|^2) e^{i\alpha_2} + \sqrt{1 + \frac{\Delta m_{\text{atm}}^2}{m_1^2}} |U_{e3}|^2 e^{i\alpha_3} \right|. \quad (86)$$

If  $CP$  is conserved, there are several different possibilities for the values of the relative  $CP$  parities of the three Majorana neutrinos  $\nu_{1,2,3}$ .

*Case A.* The three neutrinos  $\nu_{1,2,3}$  have the same  $CP$  parities,  $\phi_1 = \phi_2 = \phi_3$  (i.e.,  $\alpha_{21} = \alpha_{31} = 0$ ). The effective Majorana mass  $|\langle m \rangle|$  is given by

$$|\langle m \rangle| \cong m_1 \left( 1 - |U_{e3}|^2 + \sqrt{1 + \frac{\Delta m_{\text{atm}}^2}{m_1^2}} |U_{e3}|^2 \right). \quad (87)$$

Note that (in the approximation we are working)  $|\langle m \rangle|$  does not depend on the value of  $\theta_{\odot}$ . Therefore, for all analyses of the solar neutrino data  $|\langle m \rangle|$  is bounded to lie in the interval

$$2.0 \times 10^{-2} \text{ eV} \leq |\langle m \rangle| \leq 2.0 \times 10^{-1} \text{ eV}. \quad (88)$$

These values of  $|\langle m \rangle|$  can be probed in the future  $(\beta\beta)_{0\nu}$ -decay experiments [31–34].

*Case B.* If  $\phi_1 = \phi_2 = -\phi_3$  (i.e.,  $\alpha_{21} = 0$ ,  $\alpha_{31} = \pm\pi$ ),  $|\langle m \rangle|$  has the form

$$|\langle m \rangle| \cong m_1 \left( 1 - |U_{e3}|^2 - \sqrt{1 + \frac{\Delta m_{\text{atm}}^2}{m_1^2}} |U_{e3}|^2 \right). \quad (89)$$

The three terms in the brackets in Eq. (89) can mutually compensate each other if  $|U_{e3}|^2$  has a value determined by the condition

$$|U_{e3}|_0^2 = \frac{1}{1 + \sqrt{\frac{\Delta m_{\text{atm}}^2}{m_1^2}}}. \quad (90)$$

Using  $\max(\Delta m_{\text{atm}}^2) = 8 \times 10^{-3} \text{ eV}^2$  [see Eq. (5)] and  $\min(m_1) = 0.02 \text{ eV}$ , we find that the term on the right-hand side of Eq. (77),  $(1 + \sqrt{\Delta m_{\text{atm}}^2/m_1^2})^{-1} \geq 0.18$ . Thus, condition (90) cannot be satisfied by the experimentally allowed values of  $|U_{e3}|^2$ . Correspondingly, cancellation in Eq. (89) is impossible and there exists a nontrivial lower bound on  $|\langle m \rangle|$ :

$$1.6(1.5) \times 10^{-2} \text{ eV} \leq |\langle m \rangle| \leq 2.0(2.0) \times 10^{-1} \text{ eV}. \quad (91)$$

The predictions for  $|\langle m \rangle|$  in this case can be tested in the next generation of  $(\beta\beta)_{0\nu}$ -decay experiments as well.

The dependence of  $|\langle m \rangle|$  on  $|U_{e3}|^2$  for  $\phi_1 = \phi_2 = \phi_3$  and  $\phi_1 = \phi_2 = -\phi_3$  is shown in Fig. 17. The figure is obtained for the 90% (99%) C.L. results of the analysis of Ref. [58] and taking into account the dependence of the allowed values of  $\Delta m_{\text{atm}}^2$  on the value of  $|U_{e3}|^2$ . Since in both cases  $|\langle m \rangle|$  does not depend on  $\theta_{\odot}$  and  $\Delta m_{\odot}^2$ , the results exhibited in Fig. 17 are valid for all the different solutions of the solar neutrino problem.

*Case C.* For  $\phi_1 = -\phi_2 = \phi_3$  (i.e.,  $\alpha_{21} = \pm\pi$ ,  $\alpha_{31} = 0$ ), the effective mass  $|\langle m \rangle|$  is given by

$$|\langle m \rangle| \cong m_1 \left| \cos 2\theta_{\odot} (1 - |U_{e3}|^2) + \sqrt{1 + \frac{\Delta m_{\text{atm}}^2}{m_1^2}} |U_{e3}|^2 \right|. \quad (92)$$

Now  $|\langle m \rangle|$  depends on  $\cos 2\theta_{\odot}$  and we will get different predictions for  $|\langle m \rangle|$  for the different solutions of the solar neutrino problem. Since for the SMA solution one has  $\cos 2\theta_{\odot} \cong 1$ , the results for  $|\langle m \rangle|$  corresponding to the SMA solution practically coincide with those in case (1) considered above and given in Eq. (88). According to the 99% C.L. results of Ref. [58], for the LMA and LOW-QVO solutions  $\cos 2\theta_{\odot}$  can be either positive or negative and therefore there can be a cancellation for any allowed value of  $|U_{e3}|^2$ . The intervals of allowed values of  $|\langle m \rangle|$  read

$$2.2 \times 10^{-3} (0.0) \text{ eV} \leq |\langle m \rangle| \leq 1.3 (1.4) \times 10^{-1} \text{ eV}, \quad \text{LMA}, \quad (93)$$

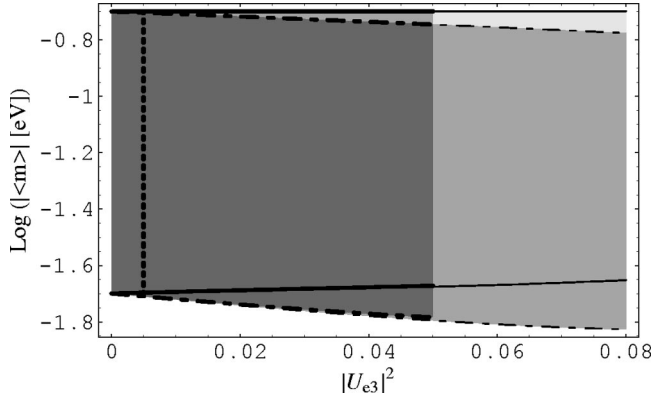


FIG. 17. The effective Majorana mass  $|\langle m \rangle|$ , allowed by the data from the solar and atmospheric neutrino and CHOOZ experiments, as a function of  $|U_{e3}|^2$  in the case of partial hierarchy mass spectrum, Eq. (84). The values of  $|\langle m \rangle|$  are obtained for  $\Delta m_{\odot}^2$ , and  $\sin^2 \theta_{\odot}$  from the LMA MSW solution region and  $\Delta m_{\text{atm}}^2$  and  $|U_{e3}|^2$ , derived in [58] at 90% C.L. (medium-gray and dark-gray regions at  $|U_{e3}|^2 < 0.05$ ), and at 99% C.L. (light-, medium-, and dark-gray regions at  $|U_{e3}|^2 < 0.08$ ). The 90% (99%) C.L. allowed regions located (i) between the two thick (thin) solid lines and (ii) between the two thick (thin) dashed lines correspond to the two cases of  $CP$  conservation: (i)  $\phi_1 = \phi_2 = \phi_3$  and (ii)  $\phi_1 = \phi_2 = -\phi_3$ ,  $i\phi_{2,3}$  being the  $CP$  parities of  $\nu_{2,3}$ . The values of  $|\langle m \rangle|$ , calculated for the best fit values of  $\Delta m_{\odot}^2$ ,  $\Delta m_{\text{atm}}^2$ ,  $\sin^2 \theta_{\odot}$ ,  $|U_{e3}|^2$ , and for  $0.02 \text{ eV} \leq m_1 \leq 0.2 \text{ eV}$  are indicated by the thick dotted line.

$$0 \leq |\langle m \rangle| \leq 7.0 \text{ (11)} \times 10^{-2} \text{ eV},$$

LOW-QVO, (94)

$$2.0 \text{ (2.0)} \times 10^{-2} \text{ eV} \leq |\langle m \rangle| \leq 2.0 \text{ (2.0)} \times 10^{-1} \text{ eV}, \quad \text{SMA.} \quad (95)$$

Since for the LMA solution the corrections  $\sim \Delta m_{21}^2/m_1^2 = \Delta m_{\odot}^2/m_1^2$  can be as large as  $\sim 2.3 \times 10^{-3} \text{ eV}$ , the (99% C.L.) lower limit,  $\min(|\langle m \rangle|) = 0 \text{ eV}$ , quoted above, can actually be any value between  $\sim 2.3 \times 10^{-3} \text{ eV}$  and  $0 \text{ eV}$ . In contrast, from the analysis of Ref. [7] it follows that  $\cos 2\theta_{\odot} > 0$  for the LMA and LOW-QVO solutions. Thus, according to the results of [7], cancellation of the two contributions in Eq. (92) is excluded for both the LMA and LOW-QVO solutions, leading to the following intervals of possible values of  $|\langle m \rangle|$ :

$$4.0 \times 10^{-3} \text{ eV} \leq |\langle m \rangle| \leq 1.4 \times 10^{-1} \text{ eV}, \quad \text{LMA,} \quad (96)$$

$$6.6 \times 10^{-3} \text{ eV} \leq |\langle m \rangle| \leq 1.2 \times 10^{-1} \text{ eV}, \quad \text{LOW-QVO.} \quad (97)$$

*Case D.* For  $\phi_1 = -\phi_2 = -\phi_3$  (i.e.,  $\alpha_{21} = \alpha_{31} = \pm \pi$ ), the expression for  $|\langle m \rangle|$  can be written as

$$|\langle m \rangle| \approx m_1 \left| \cos 2\theta_{\odot} (1 - |U_{e3}|^2) - \sqrt{1 + \frac{\Delta m_{\text{atm}}^2}{m_1^2} |U_{e3}|^2} \right|. \quad (98)$$

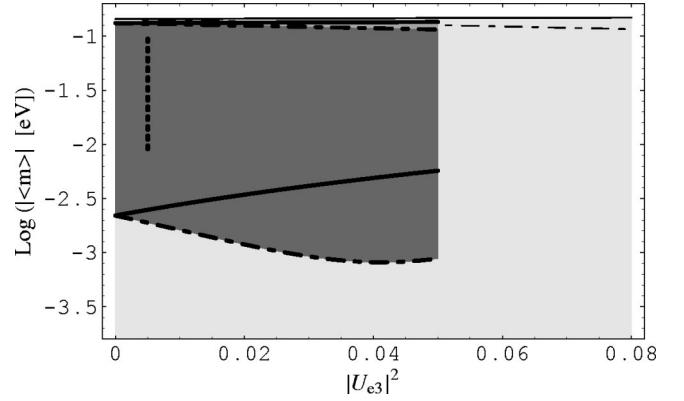


FIG. 18. The same as Fig. 17 but for two different sets of values of the relative  $CP$  parities of the massive Majorana neutrinos. The allowed regions are derived using the results of [58] at 90% C.L. (medium-gray and dark-gray regions at  $|U_{e3}|^2 < 0.05$ ) and at 99% C.L. (light-, medium-, and dark-gray regions at  $|U_{e3}|^2 < 0.08$ ). The 90% (99%) C.L. allowed regions located (i) between the two thick solid lines (between the thin solid line and the horizontal axis) and (ii) between the two thick dashed lines (between the thin dashed line and the horizontal axis) correspond to the two cases of  $CP$  conservation: (i)  $\phi_1 = -\phi_2 = \phi_3$  and (ii)  $\phi_1 = -\phi_2 = -\phi_3$ ,  $i\phi_{2,3}$  being the  $CP$  parities of  $\nu_{2,3}$ . The values of  $|\langle m \rangle|$ , calculated for the best fit values of  $\Delta m_{\odot}^2$ ,  $\Delta m_{\text{atm}}^2$ ,  $\sin^2 \theta_{\odot}$ ,  $|U_{e3}|^2$ , and for  $0.02 \text{ eV} \leq m_1 \leq 0.2 \text{ eV}$  are indicated by the thick dotted line.

Most of the observations made for the previous case hold also for this one. The results obtained in Ref. [58] imply the following allowed intervals of values of  $|\langle m \rangle|$ :

$$8.0 \times 10^{-4} \text{ (0.0)} \text{ eV} \leq |\langle m \rangle| \leq 1.2 \text{ (1.3)} \times 10^{-1} \text{ eV}, \quad \text{LMA,} \quad (99)$$

$$0 \leq |\langle m \rangle| \leq 5.0 \text{ (14)} \times 10^{-2} \text{ eV},$$

LOW-QVO, (100)

$$1.6 \text{ (1.5)} \times 10^{-2} \text{ eV} \leq |\langle m \rangle| \leq 2.0 \text{ (2.0)} \times 10^{-1} \text{ eV}, \quad \text{SMA.} \quad (101)$$

The dependence of  $|\langle m \rangle|$  on  $|U_{e3}|^2$  for the two cases  $\phi_1 = -\phi_2 = \pm \phi_3$  is shown in Figs. 18 and 19, respectively. The 90% and 99% C.L. results of Ref. [58] were used for the figures (in particular, the dependence of  $\Delta m_{\text{atm}}^2$  and  $\theta_{\odot}$  on  $|U_{e3}|^2$  was taken into account).

In order to illustrate the dependence of  $|\langle m \rangle|$  on  $\theta_{\odot}$ , we plot in Fig. 20 the ratio  $|\langle m \rangle|/m_1$  versus  $\cos 2\theta_{\odot}$  for the four  $CP$ -conserving cases discussed above. The region marked with dark-gray scale corresponds to “just- $CP$ -violation.” A value of  $|\langle m \rangle|/m_1$  in this region would signal the existence of  $CP$  violation in the leptonic sector, induced by the Majorana  $CP$ -violating phases:  $|\langle m \rangle|/m_1$  cannot take a value in the indicated region if  $CP$  parity is conserved.

Note that, as we have shown in Sec. V, if the neutrino mass spectrum is of the inverted hierarchy type, one typically has  $\max(|\langle m \rangle|) \leq 0.06 \text{ eV}$ , with the largest allowed value of  $|\langle m \rangle| \leq (0.08-0.09) \text{ eV}$  possible only in the case of the SMA solution of the  $\nu_{\odot}$  problem. This has to be com-

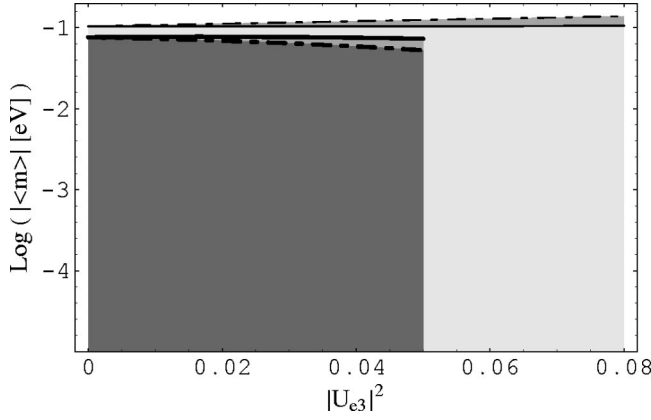


FIG. 19. The same as in Fig. 18 but for the LOW-QVO solution of the solar neutrino problem. The 90% (99%) C.L. allowed regions located (i) between the thick (thin) solid line and the horizontal axis and (ii) between the thick (thin) dashed line and the horizontal axis correspond to the two cases of  $CP$  conservation: (i)  $\phi_1 = -\phi_2 = \phi_3$ , and (ii)  $\phi_1 = -\phi_2 = -\phi_3$ ,  $i\phi_{2,3}$  being the  $CP$  parities of  $\nu_{2,3}$ .

pared with  $\max(|\langle m \rangle|) = \max(m_1) \cong 0.2$  eV one finds for the partial mass hierarchy spectrum under study.

If the  $CP$  symmetry is violated, the two  $CP$ -violating phases entering into the expression (86) for  $|\langle m \rangle|$ ,  $\alpha_{21}$  and  $\alpha_{31}$ , must obey the following relation:

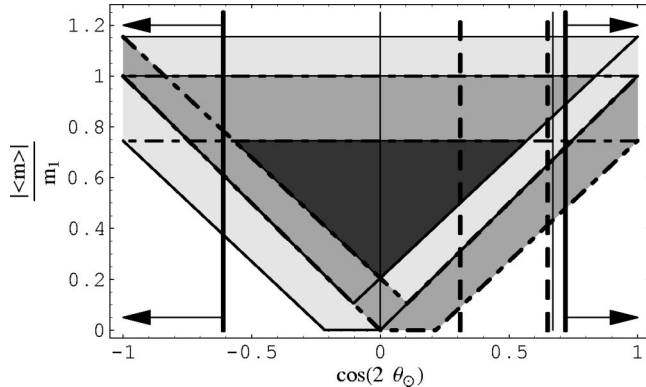


FIG. 20. The dependence of  $|\langle m \rangle|/m_1$  on  $\cos 2\theta_\odot$  for the partial hierarchy mass spectrum, Eq. (84), and the LMA solution of the  $\nu_\odot$  problem, for the 99% C.L. allowed values of the solar and atmospheric neutrino oscillation parameters and  $0.02 \text{ eV} \leq m_1 \leq 0.2$  eV. If  $CP$  invariance holds, the values of  $|\langle m \rangle|/m_1$  lie (i) for  $\phi_1 = \phi_2 = \phi_3$ , in the region between the two thin solid horizontal lines (in light and medium gray), (ii) for  $\phi_1 = \phi_2 = -\phi_3$ , in the region between the two thick horizontal dash-dotted lines (in light-gray and medium-gray colors), (iii) for  $\phi_1 = -\phi_2 = +\phi_3$ , in the light and medium gray polygon with solid-line contours, and (iv) for  $\phi_1 = -\phi_2 = -\phi_3$ , in the medium-gray polygon with the dash-dotted-line contours. The “just- $CP$ -violation” region is denoted by dark-gray color. The values of  $\cos 2\theta_\odot$  between the doubly thick solid, the normal solid, and the doubly thick dashed lines correspond to the 99%, 99%, and 95% C.L. LMA solution regions in Refs. [58], [56], and [7], respectively.

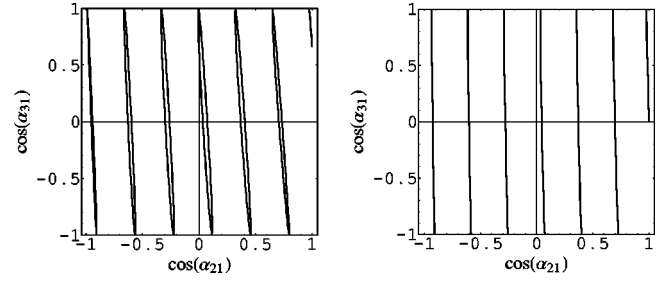


FIG. 21. The interdependence of the two  $CP$ -violating phases  $\alpha_{21}$  and  $\alpha_{31}$  for a given value of the ratio  $|\langle m \rangle|/m_1$  in the case of a partially hierarchical neutrino mass spectrum. The figures are obtained for  $|\langle m \rangle| = \sqrt{1 + 0.5n} \times 10^{-2}$  eV with  $n=0,1,\dots,6$  (with increasing  $|\langle m \rangle|$  from left to right), the best fit values of the solar and atmospheric neutrino oscillation parameters from [58], quoted in Sec. II, and  $m_1=0.02$  eV (left-hand plot), and for  $|\langle m \rangle| = \sqrt{0.5n} \times 10^{-1}$  eV with  $n=0,1,\dots,6$  (with increasing  $|\langle m \rangle|$  from left to right), the best fit values of the solar and atmospheric neutrino oscillation parameters from [58], and  $m_1=0.2$  eV (right-hand plot). The values of  $\cos \alpha_{21,31}=0, \pm 1$ , correspond to  $CP$  invariance.

$$\begin{aligned}
 & |\langle m \rangle|^2 - m_1^2 \cos^4 \theta_\odot (1 - |U_{e3}|^2)^2 - m_1^2 \sin^4 \theta_\odot (1 - |U_{e3}|^2)^2 \\
 & - (m_1^2 + \Delta m_{\text{atm}}^2) |U_{e3}|^4 \\
 & = 2m_1^2 \cos^2 \theta_\odot \sin^2 \theta_\odot (1 - |U_{e3}|^2)^2 \cos \alpha_{21} \\
 & + 2m_1 \sqrt{m_1^2 + \Delta m_{\text{atm}}^2} \cos^2 \theta_\odot |U_{e3}|^2 (1 - |U_{e3}|^2) \cos \alpha_{31} \\
 & + 2m_1 \sqrt{m_1^2 + \Delta m_{\text{atm}}^2} \sin^2 \theta_\odot |U_{e3}|^2 (1 - |U_{e3}|^2) \\
 & \times (\cos \alpha_{21} \cos \alpha_{31} + \sin \alpha_{21} \sin \alpha_{31}). \quad (102)
 \end{aligned}$$

One could constrain  $\alpha_{21}$  and  $\alpha_{31}$  once the values of all other observables in Eq. (102) are measured with a sufficiently good precision. In Figs. 21 and 22 we illustrate this possibility by plotting  $\cos \alpha_{21}$  versus  $\cos \alpha_{31}$  for the best fit values of  $\Delta m_{\odot}^2$ ,  $\theta_\odot$ ,  $\Delta m_{\text{atm}}^2$ , and  $|U_{e3}|^2$  found in [58] (see Sec. II),

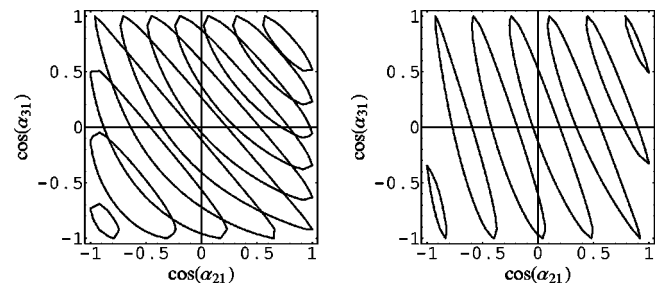


FIG. 22. The same as in Fig. 21 but for  $|\langle m \rangle| = \sqrt{0.5n} \times 10^{-1}$  eV with  $n=1,\dots,10$  (with increasing  $|\langle m \rangle|$  from left to right),  $|U_{e3}|^2=0.08$ , the best fit values of the other solar and atmospheric neutrino oscillation parameters from [58], quoted in Sec. II, and  $m_1=0.02$  eV (left-hand plot), and for  $|\langle m \rangle| = \sqrt{1 + 0.5n} \times 10^{-2}$  eV with  $n=0,1,\dots,6$  (with increasing  $|\langle m \rangle|$  from left to right),  $|U_{e3}|^2=0.08$ , the best fit values of the other solar and atmospheric neutrino oscillation parameters from [58], and  $m_1=0.2$  eV (right-hand plot). The values of  $\cos \alpha_{21,31}=0, \pm 1$ , correspond to  $CP$  invariance.

$m_1 = 0.02, 0.2$  eV, and for  $|U_{e3}|^2 = 0.08$ , best fit values of the remaining three parameters and  $m_1 = 0.02, 0.2$  eV, respectively. Let us note, however, that obtaining experimental information about the mass  $m_1$  ( $\approx m_2$ ), which in the case under study is supposed to have a value  $\sim (0.02-0.20)$  eV, seems at present to be extremely difficult.

### B. Spectrum with partial inverted hierarchy

In this case  $|U_{e1}|^2 = \sin^2 \theta$  and is constrained by the CHOOZ limit. The general expression for  $\langle m \rangle$  has the form

$$\begin{aligned}
 \langle m \rangle &= |m_1| |U_{e1}|^2 e^{i\alpha_1} + (1 - |U_{e1}|^2) \\
 &\times \sqrt{m_1^2 + \Delta m_{\text{atm}}^2} (\cos^2 \theta_\odot + \sin^2 \theta_\odot e^{i(\alpha_3 - \alpha_2)}) e^{i\alpha_2}.
 \end{aligned}
 \quad (103)$$

For relatively small values of  $|U_{e1}|^2$ , e.g.,  $|U_{e1}|^2 \leq 0.01$ , the term  $m_1 |U_{e1}|^2 \leq 2 \times 10^{-3}$  eV and neglecting it we get the following simple expression for  $\langle m \rangle$ :

$$\langle m \rangle \cong |\cos^2 \theta_\odot + \sin^2 \theta_\odot e^{i(\alpha_3 - \alpha_2)}| \sqrt{m_1^2 + \Delta m_{\text{atm}}^2}. \quad (104)$$

In the  $CP$ -conserving case, there are two major possibilities for the values of the neutrino  $CP$  parities.

*Case A.* If  $\phi_2 = \phi_3 = \pm \phi_1$  (i.e.,  $\alpha_{21} = \alpha_{31} = 0, \pm \pi$ ), the effective Majorana mass parameter  $\langle m \rangle$  is given by

$$\langle m \rangle = \sqrt{m_1^2 + \Delta m_{\text{atm}}^2} (1 - |U_{e1}|^2) \pm m_1 |U_{e1}|^2, \quad (105)$$

where  $m_1 |U_{e1}|^2 \leq 1.8 \times 10^{-2}$  eV. A cancellation between the two terms in Eq. (105) is impossible and one has a nontrivial lower bound on  $\langle m \rangle$ . The allowed values of  $\langle m \rangle$  do not depend on  $\theta_\odot$  and therefore are the same for all solutions of the  $\nu_\odot$  problem and the different analyses of the solar neutrino data. They depend very weakly on  $|U_{e1}|^2$ . We have

$$2.8 \text{ (1.8)} \times 10^{-2} \text{ eV} \leq \langle m \rangle \leq 2.1 \text{ (2.2)} \times 10^{-1} \text{ eV}.$$

*Case B.* For  $\phi_2 = -\phi_3 = \pm \phi_1$  [i.e.,  $(\alpha_3 - \alpha_2) = \pm \pi$ ,  $\alpha_{21}, \alpha_{31} = 0, \pm \pi$ ],  $\langle m \rangle$  takes the form

$$\langle m \rangle_\pm = |\cos 2\theta_\odot \sqrt{m_1^2 + \Delta m_{\text{atm}}^2} (1 - |U_{e1}|^2) \pm m_1 |U_{e1}|^2|. \quad (106)$$

For the SMA solution we have  $\cos 2\theta_\odot \cong 1$  and the results for  $\langle m \rangle$  are equivalent to those in the case (1). For the LMA and LOW-QVO solutions the values  $\langle m \rangle$  depend on the solution and on the data analysis. In Figs. 23 and 24 we plot the allowed regions of values of  $\langle m \rangle$  versus  $\Delta m_{\text{atm}}^2$  for the LMA and LOW-QVO solutions, respectively, of Ref. [58]. Since for both solutions values of  $|\cos 2\theta_\odot| < 0.09$  are possible (at 90% and 99% C.L.) [58], and we can have also  $|U_{e1}|^2 \cong 0$ , one does not get a significant lower bound on  $\langle m \rangle$ . The values of  $\langle m \rangle$ , corresponding to the three solutions of the solar neutrino problem and the different data analyses in [7], [56], and [58], are reported in Table VI. According to the analysis of Ref. [7],  $\cos 2\theta_\odot > 0.2$  (0.4) for the LMA (LOW-QVO) solution. This leads to the nontrivial

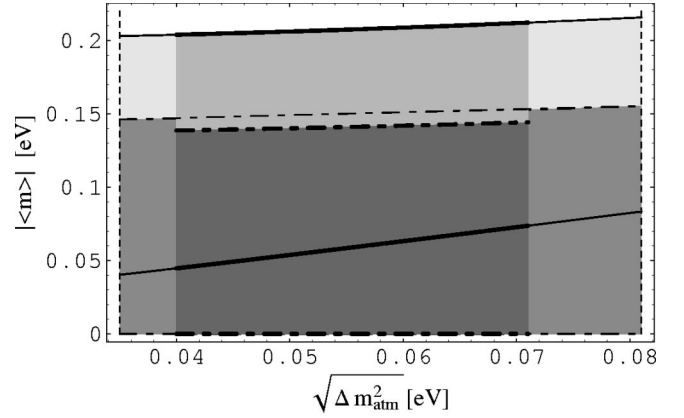


FIG. 23. The effective Majorana mass  $\langle m \rangle$  as a function of  $\sqrt{\Delta m_{\text{atm}}^2}$  for the neutrino mass spectrum of the partial inverted hierarchy type, Eq. (85). The allowed regions (in gray) correspond to the LMA solution of Ref. [58]. In the case of  $CP$  invariance and for the 90% (99%) C.L. solution regions,  $\langle m \rangle$  can have values (i) for  $\phi_2 = \phi_3$ , in the medium-light and dark-gray (light-gray, medium-light, medium-dark-gray, and dark-gray) upper regions, delimited by the doubly thick (thick and doubly thick) solid lines, and (ii) for  $\phi_2 = -\phi_3$ , in the dark-gray (medium-light-gray, medium-dark-gray, and dark-gray) region limited by the doubly thick (thick and doubly thick) dash-dotted lines. If  $CP$  is not conserved,  $\langle m \rangle$  can lie in any of the regions marked by different gray scales.

lower bounds on the possible values of  $\langle m \rangle$  for the indicated solutions, cited in Table VI.

The dependence of  $\langle m \rangle$  on  $\cos 2\theta_\odot$  is exhibited in Fig. 25. The uncertainty in the allowed ranges of values of  $\langle m \rangle$  is mainly due to the relatively large interval of possible values of  $m_1$  we consider.

If  $CP$  is not conserved and  $|U_{e1}|^2$  is shown to be sufficiently small, so that for  $m_1 \leq 0.2$  eV the term  $m_1 |U_{e1}|^2$  in Eq. (103) can be neglected, one has the following simple relation between  $\sin^2(\alpha_3 - \alpha_2)/2$  and the observables  $\langle m \rangle$ ,  $\sin^2 2\theta_\odot$ , and  $m_1^2 + \Delta m_{\text{atm}}^2$ :

$$\sin^2 \frac{\alpha_3 - \alpha_2}{2} = \frac{1}{\sin^2 2\theta_\odot} \left( 1 - \frac{\langle m \rangle^2}{m_1^2 + \Delta m_{\text{atm}}^2} \right). \quad (107)$$

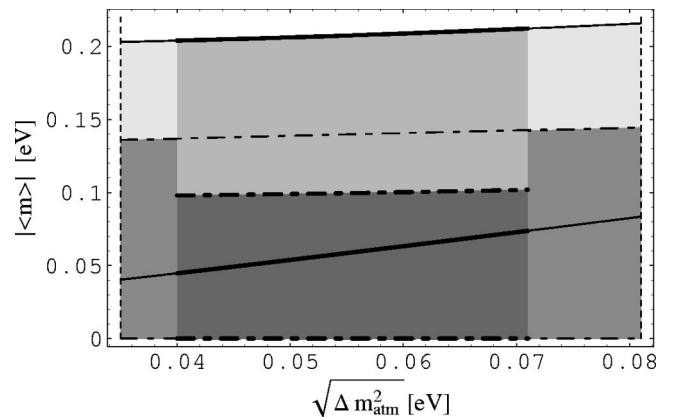


FIG. 24. The same as Fig. 23 for the 90% (99%) C.L. LOW-QVO solution of Ref. [58].

TABLE VI. Values of  $|\langle m \rangle|$ , corresponding to the different solutions of the solar neutrino problem, neutrino oscillation interpretation of the atmospheric neutrino data, and the CHOOZ limit. The results are obtained for the mass spectrum with partial inverted hierarchy, Eq. (85),  $CP$  conservation,  $\phi_2 = -\phi_3 = \pm\phi_1$ , negligible  $m_1|U_{e1}|^2$ , and  $0.02 \text{ eV} \leq m_1 \leq 0.20 \text{ eV}$  (see text for further details).

Data from		$ \langle m \rangle $ [eV]
Ref. [7]	LMA	$0 - 1.4 \times 10^{-1}$
(95% C.L.)	LOW-QVO	$1.0 \times 10^{-2} - 1.1 \times 10^{-1}$
Ref. [56]	LMA	$0 (0) \times 10^{-2} - 1.4 (1.5) \times 10^{-1}$
[90% (99%) C.L.]	SMA	$(1.8 \times 10^{-2} - 2.2 \times 10^{-1})$
	LOW-QVO	$0 (0) \times 10^{-3} - 0.5 (1.1) \times 10^{-1}$
Ref. [58]	LMA	$0 (0) - 1.4 (1.5) \times 10^{-1}$
[90 (99%) C.L.]	SMA	$2.8 (1.8) \times 10^{-2} - 2.1 (2.2) \times 10^{-1}$
	LOW-QVO	$0 (0) - 1.0 (1.4) \times 10^{-1}$

The allowed ranges of  $\sin^2(\alpha_3 - \alpha_2)/2$  as a function of  $|\langle m \rangle|/\sqrt{m_1^2 + \Delta m_{\text{atm}}^2}$  are reported in Fig. 26 for the LMA and LOW-QVO solutions [58], respectively. Obviously, knowing  $|\langle m \rangle|$ ,  $\sin^2 2\theta_\odot$  and  $(m_1^2 + \Delta m_{\text{atm}}^2)$  experimentally would allow to get information about the  $CP$  violation caused by the Majorana  $CP$ -violating phases. We note that this conclusion is not valid for the SMA solution of the solar neutrino problem since for this solution  $\sin^2 2\theta_\odot \ll 1$  and [see Eq. (104)]

$$|\langle m \rangle| \cong \sqrt{m_1^2 + \Delta m_{\text{atm}}^2}, \quad \text{SMA MSW.} \quad (108)$$

However, the measurement of  $|\langle m \rangle|$  in this case would allow to determine  $m_1$  and thus the whole neutrino mass spectrum.

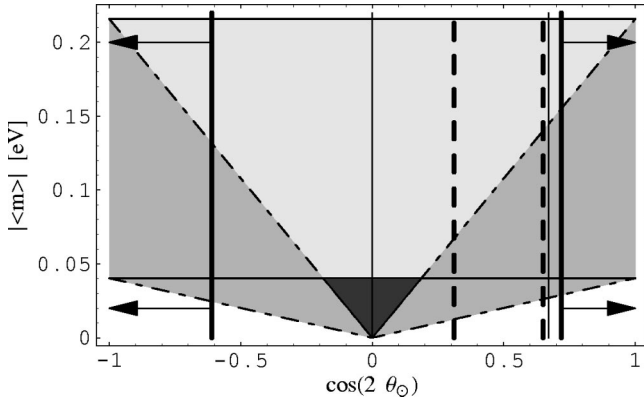


FIG. 25. The dependence of  $|\langle m \rangle|$  on  $\cos 2\theta_\odot$  for the neutrino mass spectrum with partial inverted hierarchy, Eq. (85), and the LMA solution of the  $\nu_\odot$  problem. The region between the two thick horizontal solid lines (in light-gray and medium-gray colors) and the two triangular regions between the thick dash-dotted lines (in medium-gray color) correspond to the two  $CP$ -conserving cases  $\phi_2 = \phi_3$  and  $\phi_2 = -\phi_3$ , respectively. The “just- $CP$ -violation” region is denoted by dark-gray color. The regions between each of the three pairs of vertical lines of a given type, solid, doubly thick solid, and doubly thick dashed lines, correspond to the intervals of values of  $\cos 2\theta_\odot$  for the LMA solution derived (at 99% C.L.) in Ref. [7] (region between the two doubly thick dashed lines), Ref. [56] (region between the solid lines), and Ref. [58].

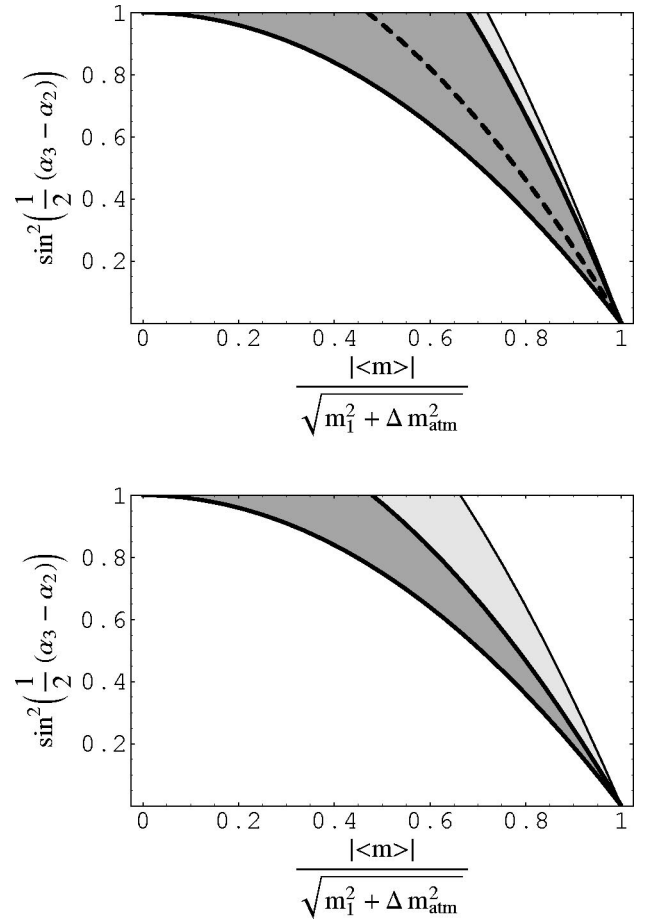


FIG. 26. The  $CP$ -violation factor  $\sin^2(\alpha_2 - \alpha_3)/2$  as a function of  $|\langle m \rangle|/\sqrt{m_1^2 + \Delta m_{\text{atm}}^2}$  in the case of a partially inverted mass hierarchy spectrum, Eq. (85), and the LMA (upper panel) and LOW-QVO (lower panel) solutions of Ref. [58], obtained at 90% C.L. (medium-gray region with thick contours) and 99% C.L. (light-gray + medium-gray region limited by ordinary solid lines). The values of  $|\langle m \rangle|$ , corresponding to the best fit values of the input parameters, found in [58], are indicated by the dashed line. A value of  $\sin^2(\alpha_2 - \alpha_3)/2 \neq 0, 1$ , would signal  $CP$  violation.

## VIII. CONCLUSIONS

Assuming three-neutrino mixing and massive Majorana neutrinos, we have studied in detail the implications of the neutrino oscillation solutions of the solar and atmospheric neutrino problems and of the data of the reactor long baseline CHOOZ and Palo Verde experiments [64,65], for the predictions of the effective Majorana mass  $|\langle m \rangle|$ , which determines the  $(\beta\beta)_{0\nu}$ -decay rate. The results of the neutrino oscillation fits of the latest solar and atmospheric neutrino data [7,55,56,58] have been used in our analysis. We have considered essentially all possible types of neutrino mass spectra compatible with the existing data: hierarchical, neutrino mass spectra with inverted hierarchy, with partial hierarchy, with partial inverted hierarchy, and with three quasi-degenerate neutrinos. In the present study we have investigated the general case of  $CP$  nonconservation. The  $(\beta\beta)_{0\nu}$ -decay effective Majorana mass  $|\langle m \rangle|$  depends, in general, on two physical (Majorana)  $CP$ -violating phases. For each of the

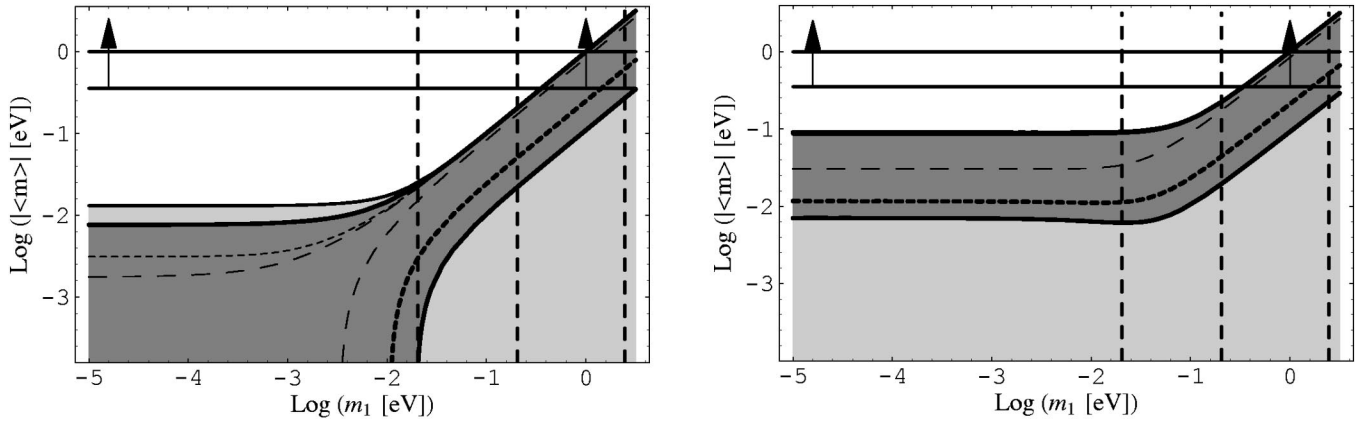


FIG. 27. The dependence of  $|\langle m \rangle|$  on  $m_1$  in the case of  $\Delta m_\odot^2 = \Delta m_{21}^2$  (left panel) and of  $\Delta m_\odot^2 = \Delta m_{32}^2$  (lower panel). For  $\Delta m_\odot^2 = \Delta m_{21}^2$  (left panel), the allowed values of  $|\langle m \rangle|$  are obtained (i) using the 99% C.L. results of Ref. [58] for the LMA solution of the  $\nu_\odot$  problem (light-gray and dark-gray regions between the thick solid line and the axes), for the LOW-QVO solution (light-gray and dark-gray regions between the thin dotted line and the axes), and for the SMA one (the dark-gray region between the thin dashed lines) and (ii) using the results of Ref. [7] for the LMA (dark-gray region between the two doubly thick solid lines) and for the LOW-QVO (dark-gray region between the upper doubly thick solid line and the doubly thick dotted line) solutions. For  $\Delta m_\odot^2 = \Delta m_{32}^2$  (right panel), the allowed values are obtained (i) using the 99% C.L. results of the analysis of Ref. [58] for the LMA and LOW-QVO solutions (light-gray and dark-gray regions between the doubly thick line and the axes) and the SMA one (the dark-gray region between the upper doubly thick line and the thin dashed one) and (ii) using the results of Ref. [7] for the LMA (dark-gray region between the two doubly thick solid lines) and the LOW-QVO (dark-gray region between the upper doubly thick solid line and the doubly thick dotted line) solutions. The regions divided by the vertical dashed lines on the left (right) panel correspond to (i)  $m_1 \leq 0.02$  eV and, if  $m_1 \leq \sqrt{\Delta m_\odot^2}$  ( $m_1 < \sqrt{\Delta m_\odot^2} \leq \sqrt{\Delta m_{atm}^2}$ ), to a hierarchical (inverted hierarchy) neutrino mass spectrum, (ii)  $0.02$  eV  $\leq m_1 \leq 0.2$  eV, i.e., a spectrum with partial hierarchy (partial inverted hierarchy), and to (iii)  $m_1 \geq 0.2$  eV, i.e., quasidegenerate neutrinos. For both cases the upper bounds from Ref. [29], Eq. (4), are shown by the horizontal upper doubly thick solid lines.

five types of neutrino mass spectra indicated above we have derived detailed predictions for the values of  $|\langle m \rangle|$  for the three solutions of the solar neutrino problem favored by the current solar neutrino data: the LMA MSW, the SMA MSW, and the LOW-QVO ones. In each of these cases we have identified the “just- $CP$ -violation” region of values of  $|\langle m \rangle|$  whenever it existed: a value of  $|\langle m \rangle|$  in this region would unambiguously signal the presence of  $CP$  violation in the lepton sector. Analyzing the case of  $CP$  conservation, we have derived predictions for  $|\langle m \rangle|$  corresponding to all possible sets of values of the relative  $CP$  parities of the three massive Majorana neutrinos. This was done for all different types of neutrino mass spectra we have considered. We have investigated the possibility of cancellation between the different terms contributing to  $|\langle m \rangle|$ . The cases when such a cancellation is impossible and there exists a nontrivial lower bound on  $|\langle m \rangle|$  were identified and the corresponding lower bounds were given.

More specifically, if the neutrino mass spectrum is hierarchical, only the contributions to  $|\langle m \rangle|$  due to the exchange of the two heavier Majorana neutrinos  $\nu_{2,3}$  can be relevant and  $|\langle m \rangle|$  depends only on one  $CP$ -violating phase  $\alpha_{32}$ . For the SMA and LOW-QVO solutions of the solar neutrino problem one has  $|\langle m \rangle| \leq 4.0 \times 10^{-3}$  eV. For the LMA solution we get  $|\langle m \rangle| \leq 8.5 \times 10^{-3}$  eV if one uses the results of the analyses in [7,56], while the results of the three-neutrino mixing analysis of [58] allow a somewhat larger value of  $|\langle m \rangle| \leq (1.0-2.0) \times 10^{-2}$  eV. The maximal values of  $|\langle m \rangle|$  correspond to  $CP$  conservation and  $\nu_2$  and  $\nu_3$  having identical  $CP$  parities,  $\phi_2 = \phi_3$ . If  $\phi_2 = -\phi_3$ , the allowed maximal

values of  $|\langle m \rangle|$  are somewhat smaller. For all three solutions there are no significant lower bounds on  $|\langle m \rangle|$ : the lower bound in any case does not exceed  $8.0 \times 10^{-4}$  eV. Deep mutual compensations between the terms contributing to  $|\langle m \rangle|$ , corresponding to the exchange of different virtual massive Majorana neutrinos, are possible. Such a cancellation can take place both if  $CP$  is not conserved and in the case of  $CP$  conservation if  $\phi_2 = -\phi_3$ . The degree of compensation depends, for given values of the solar and atmospheric neutrino oscillation parameters  $\Delta m_\odot^2$ ,  $\theta_\odot$ , and  $\Delta m_{atm}^2$ , on the value of  $|U_{e3}|^2$ , which is constrained by the CHOOZ data. The problem of compensations is most relevant in the case of the LMA MSW solution of the  $\nu_\odot$  problem, since in this case  $|\langle m \rangle|$  can have the largest possible values for the hierarchical neutrino mass spectrum. Because of the relatively large allowed ranges of values of  $\Delta m_\odot^2$ ,  $\theta_\odot$ , and  $\Delta m_{atm}^2$ , there are no “just- $CP$ -violation” regions of  $|\langle m \rangle|$ . A better determination of  $\Delta m_\odot^2$ ,  $\theta_\odot$ , and  $\Delta m_{atm}^2$  together with a sufficiently accurate measurement of  $|\langle m \rangle|$  could allow to get a direct information on the  $CP$ -violating phase  $\alpha_{32}$ . These results are summarized in Figs. 2–5.

In the case of the neutrino mass spectrum with inverted hierarchy, Eqs. (61)–(63), the dominant contributions to  $|\langle m \rangle|$  are again due to the two heavier Majorana neutrinos  $\nu_{2,3}$  and  $|\langle m \rangle|$  is determined by  $\Delta m_{atm}^2$ ,  $\sin^2 2\theta_\odot$ , the  $CP$ -violating phase  $\alpha_{32}$ , and  $|U_{e1}|^2$ , which is constrained by the CHOOZ data. The effective Majorana mass can be considerably larger than in the case of a hierarchical neutrino mass spectrum:  $|\langle m \rangle| \leq (6.8-8.9) \times 10^{-2}$  eV. The maximal

$|\langle m \rangle|$  corresponds to  $CP$  conservation and  $\phi_2 = \phi_3$  ( $\alpha_{32} = 0$ ); it is possible for all three solutions of the  $\nu_\odot$  problem. It varies weakly with the results of the different analyses being used. For  $\phi_2 = -\phi_3$  ( $\alpha_{32} = \pm\pi$ ) the maximal allowed values of  $|\langle m \rangle|$  are the same for the SMA MSW solution, while we have  $|\langle m \rangle| \leq (4.8-5.9) \times 10^{-2}$  eV [ $|\langle m \rangle| \leq (3.7-5.4) \times 10^{-2}$  eV] for the LMA MSW [LOW-QVO] solution. For all three solutions there exists a significant lower bound of  $|\langle m \rangle| \geq (3-4) \times 10^{-2}$  eV if  $\phi_2 = \phi_3$ . For  $\phi_2 = -\phi_3$  one gets an analogous lower bound only in the case of the SMA solution, while for the LMA and LOW-QVO solutions values of  $|\langle m \rangle| \ll 10^{-2}$  eV are possible. Both for the LMA and LOW-QVO solutions there exist relatively large “just- $CP$ -violation” regions of  $|\langle m \rangle|$ , in which  $|\langle m \rangle|$  has a relatively large value:  $|\langle m \rangle| \cong (2-8) \times 10^{-2}$  eV. There is no such region in the case of the SMA MSW solution. We have also shown that a sufficiently accurate measurement of  $|\langle m \rangle|$ ,  $\Delta m_{\text{atm}}^2$ ,  $\sin^2 2\theta_\odot$ , and  $(1 - |U_{e1}|^2)$  can allow us to get direct information on the value of the  $CP$ -violating phase  $\alpha_{32}$ . Our results for the case of neutrino mass spectrum with inverted hierarchy are illustrated in Figs. 6–11.

For the quasidegenerate neutrino mass spectrum, Eqs. (70)–(72), we have  $|\langle m \rangle| \sim m$ , where  $m$  is the common neutrino mass, information about which can be obtained from the  $^3\text{H}$   $\beta$ -decay experiments [67,68]:  $m < 2.5$  eV. Future astrophysical and cosmological measurements (see, e.g., [70,71]) might further constrain  $m$ . The effective Majorana mass  $|\langle m \rangle|$  depends also on  $\theta_\odot$ ,  $|U_{e3}|^2$ , which is constrained by the CHOOZ data, and on two physical  $CP$ -violating phases  $\alpha_{21}$  and  $\alpha_{31}$ . The maximal value of  $|\langle m \rangle|$  is determined by the value of  $m$ ,  $|\langle m \rangle| \leq m$ . It is possible for all three solutions of the solar neutrino problem. Obviously,  $|\langle m \rangle|$  is limited by the upper bounds obtained in the  $^3\text{H}$   $\beta$ -decay [67,68] and in the  $(\beta\beta)_{0\nu}$ -decay [29,30] [see Eqs. (3) and (4)] experiments:  $|\langle m \rangle| < (0.33-1.05)$  eV. If  $CP$  invariance holds and the  $CP$ -parities of the three massive Majorana neutrinos satisfy the relation  $\phi_1 = \phi_2 = \pm\phi_3$ , we have  $0.8m \leq |\langle m \rangle| \leq m$ . We get a similar result for  $\phi_1 = -\phi_2 = \pm\phi_3$  in the case of the SMA solution. The existence of a significant lower bound on  $|\langle m \rangle|$  for the LMA and the LOW-QVO solutions if  $\phi_1 = -\phi_2 = \pm\phi_3$  depends on the  $\min|\cos 2\theta_\odot|$ . The latter varies with the analysis: using the results of [7] one finds  $|\langle m \rangle| \geq (0.1-0.2)m$  [ $|\langle m \rangle| \geq (0.2-0.3)m$ ] for the LMA [LOW-QVO] solution. According to the (99% C.L.) results of the analysis [56,58] one can have  $\cos 2\theta_\odot = 0$  and therefore there is no significant lower bound on  $|\langle m \rangle|$  for both solutions. There exist “just- $CP$ -violation” regions for the LMA and LOW-QVO solutions, in which  $|\langle m \rangle|$  can be in the range of sensitivity of the future  $(\beta\beta)_{0\nu}$ -decay experiments, while in the case of the SMA MSW solution there is no such region. The knowledge of  $|\langle m \rangle|$ ,  $m$ ,  $\theta_\odot$ , and  $|U_{e3}|^2$  would imply a nontrivial constraint on the two  $CP$ -violating phases  $\alpha_{21}$  and  $\alpha_{31}$ . Some of our results for the quasidegenerate neutrino mass spectrum are presented graphically in Figs. 12–16.

We have analyzed also in detail the predictions for  $|\langle m \rangle|$  in the case of a neutrino mass spectrum with partial mass hierarchy, Eq. (83), and with partial inverted mass hierarchy,

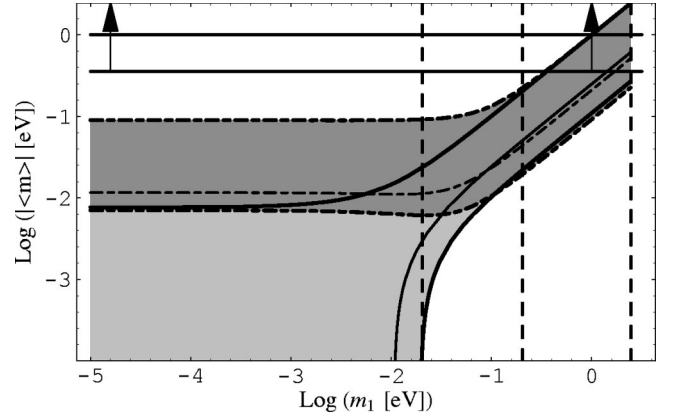


FIG. 28. The dependence of  $|\langle m \rangle|$  on  $m_1$  (i) for  $\Delta m_\odot^2 = \Delta m_{21}^2$  and using the results of the analysis of Ref. [7] for the LMA solution (light-gray and dark-gray regions between the two doubly thick solid lines) and for the LOW-QVO solution (light-gray and dark-gray regions between the upper doubly thick solid line and the thick solid line) and (ii) for  $\Delta m_\odot^2 = \Delta m_{32}^2$  and in the case of the LMA solution (dark-gray region between the two doubly thick dash-dotted lines) and the LOW-QVO solution (dark-gray region between the upper doubly thick dashed-dotted line and the thick dashed-dotted line). The upper bounds on  $|\langle m \rangle|$  from Ref. [29], Eq. (4), are shown by the horizontal upper doubly thick solid lines. The regions separated by the vertical dashed lines correspond to (i)  $m_1 \ll 0.02$  eV and, if  $m_1 \ll \sqrt{\Delta m_\odot^2}$  ( $m_1 < \sqrt{\Delta m_\odot^2} \ll \sqrt{\Delta m_{\text{atm}}^2}$ ), to a hierarchical (inverted hierarchy) neutrino mass spectrum, (ii)  $0.02$  eV  $\leq m_1 \leq 0.2$  eV, i.e., partial hierarchy and partial inverted hierarchy spectrum, and to (iii) the  $m_1 \geq 0.2$  eV, i.e., quasidegenerate spectrum.

Eq. (84). These spectra interpolate, respectively, between the hierarchical and the inverted mass hierarchy spectra and the quasidegenerate one. Accordingly, the results for  $|\langle m \rangle|$  we have found in the case of a neutrino mass spectrum with partial hierarchy (partial inverted hierarchy) “interpolate” between the results for the hierarchical (inverted mass hierarchy) and the quasidegenerate neutrino mass spectra. Most of these results are presented graphically in Figs. 17–26.

The quasidegenerate three-neutrino mass spectrum can be critically tested in the future  $^3\text{H}$   $\beta$ -decay experiment KATRIN [69], which is planned to have a sensitivity to  $m_{\nu_e} \geq 0.35$  eV. For the quasidegenerate spectrum one finds  $m_{\nu_e} = m \geq 0.20$  eV, while for all the other three-neutrino mass spectra compatible with the neutrino mass and neutrino oscillations data, we have  $m_{\nu_e} \leq 0.20$  eV.

Actually, the five different types of possible neutrino mass spectra we have considered correspond, once  $\Delta m_\odot^2$  and  $\Delta m_{\text{atm}}^2$  are known and the choice  $\Delta m_\odot^2 = \Delta m_{21}^2$  or  $\Delta m_\odot^2 = \Delta m_{32}^2$  is made, to different ranges of values of the smallest neutrino mass  $m_1$ . At the same time  $|\langle m \rangle|$  is a continuous function of  $m_1$ . In Figs. 27 and 28 we show the possible magnitude of  $|\langle m \rangle|$  as a function of  $m_1$  for  $m_1$  varying continuously<sup>8</sup> from  $10^{-5}$  eV to 2.5 eV. The results presented

<sup>8</sup>Similar plots were proposed also in Refs. [51,52].



in Figs. 27 and 28 are derived for the allowed regions of values of the relevant input oscillation parameters, obtained in [7,55,64] and in [58], and for the two possible choices of  $\Delta m_{\odot}^2$  in the case of three-neutrino mixing,  $\Delta m_{\odot}^2 = \Delta m_{21}^2$  and  $\Delta m_{\odot}^2 = \Delta m_{32}^2$ . With the notation we use, we can have  $\Delta m_{\odot}^2 = \Delta m_{21}^2$  ( $\Delta m_{\odot}^2 = \Delta m_{32}^2$ ) in the cases of hierarchical (inverted hierarchy), partial hierarchy (partial inverted hierarchy), and quasidegenerate neutrino mass spectra.

To conclude, we have found that observation of  $(\beta\beta)_{0\nu}$  decay with a rate corresponding to  $|\langle m \rangle| \geq 0.02$  eV, which is in the range of sensitivity of future  $(\beta\beta)_{0\nu}$ -decay experiments, can provide unique information on the neutrino mass spectrum. Combined with information on the lightest neutrino mass or the type of neutrino mass spectrum, it can give also information on  $CP$  violation in the lepton sector and, if  $CP$ -invariance holds, on the relative  $CP$  parities of the massive Majorana neutrinos. A measured value of  $|\langle m \rangle| \geq (2-3) \times 10^{-2}$  eV would strongly disfavor (if not rule out), under the general assumptions of the present study [three-neutrino mixing,  $(\beta\beta)_{0\nu}$  decay generated only by the charged  $(V-A)$  current weak interaction via the exchange of the three Majorana neutrinos, neutrino oscillation solutions of the solar neutrino problem, and atmospheric neutrino anomaly], the possibility of a hierarchical neutrino mass spectrum, while a value of  $|\langle m \rangle| \geq (2-3) \times 10^{-1}$  eV would rule out the hierarchical neutrino mass spectrum, strongly

disfavor the spectrum with inverted mass hierarchy, and favor the quasidegenerate spectrum.

In the present article we have considered only the mixing of three massive Majorana neutrinos. We have assumed that  $(\beta\beta)_{0\nu}$  decay is induced by the  $(V-A)$  charged current weak interaction via the exchange of massive Majorana neutrinos between two neutrons in the initial nucleus. Results for the case of four-neutrino mixing will be presented elsewhere [54].

*Note added.* Our attention was brought to Ref. [79] which discusses some of the questions studied in the present article and which appeared while the present article was being prepared for submission for publication.

## ACKNOWLEDGMENTS

We would like to acknowledge discussions with L. Wolfenstein, B. Kayser, J. Nieves, and P. Pal concerning the Majorana  $CP$ -violating phases. S.M.B. would like to thank the Elementary Particle Theory Sector at SISSA for kind hospitality and support. S.T.P. would like to acknowledge the hospitality of the Aspen Center for Physics where part of this work was done. The work of S.T.P. was supported in part by the EEC grant ERBFMRXCT960090 and by the Italian MURST under the program “Fisica Teorica delle Interazioni Fondamentali.”

- 
- [1] Super-Kamiokande Collaboration, Y. Fukuda *et al.*, Phys. Rev. Lett. **81**, 1562 (1998).
- [2] Homestake Collaboration, K. Lande, talk given at “Neutrino 2000,” 19th International Conference on Neutrino Physics and Astrophysics, Sudbury, Canada, 2000.
- [3] Kamiokande Collaboration, Y. Fukuda *et al.*, Phys. Rev. Lett. **77**, 1683 (1996).
- [4] SAGE Collaboration, J. N. Abdurashitov *et al.*, Phys. Rev. C **60**, 055801 (1999); V. Gavrin, talk given at “Neutrino 2000” [2].
- [5] GALLEX Collaboration, W. Hampel *et al.*, Phys. Lett. B **447**, 127 (1999).
- [6] Super-Kamiokande Collaboration, Y. Fukuda *et al.*, Phys. Rev. Lett. **82**, 2430 (1999).
- [7] Super-Kamiokande Collaboration, Y. Suzuki, talk given at “Neutrino 2000” [2].
- [8] GNO Collaboration, M. Altmann *et al.*, Phys. Lett. B **490**, 16 (2000); E. Bellotti, talk given at “Neutrino 2000” [2].
- [9] SNO Collaboration, A. Hallin *et al.*, Nucl. Phys. **A663-664**, 787 (2000).
- [10] J. N. Bahcall, M. H. Pinsonneault, and S. Basu, astro-ph/0010346.
- [11] LSND Collaboration, G. Mills, talk given at “Neutrino 2000” [2].
- [12] K2K Collaboration, Y. Oyama *et al.*, hep-ex/9803014; K. Nakamura, talk given at “Neutrino 2000” [2]; K2K Web page: <http://pnahep.kek.jp/>
- [13] MINOS Collaboration, P. Adamson *et al.*, NuMI-L-476, 1999; Web page: <http://www.-hep.anl.gov/ndk/hypertext/numi.html>
- [14] A. Ereditato, talk presented at the NOW2000, Otranto, Italy, 2000 (<http://www.ba.infn.it/~now2000>).
- [15] Borexino Collaboration, G. Ranucci, talk given at “Neutrino 2000” [2].
- [16] KamLAND Collaboration, A. Piepke, talk given at “Neutrino 2000” [2].
- [17] MiniBooNE Collaboration, A. Bazarko, talk given at “Neutrino 2000” [2].
- [18] S. Geer, Phys. Rev. D **57**, 6989 (1998); **59**, 039903(E) (1999); A. De Rujula, M. B. Gavela, and P. Hernandez, Nucl. Phys. **B547**, 21 (1999); K. Dick, M. Freund, M. Lindner, and A. Romanino, *ibid.* **B562**, 29 (1999); M. Campanelli, A. Bueno, and A. Rubbia, hep-ph/9905240; V. Barger, S. Geer, and K. Whisnant, Phys. Rev. D **61**, 053004 (2000); A. Donini, M. B. Gavela, P. Hernandez, and S. Rigolin, Nucl. Phys. **B574**, 23 (2000); A. Romanino, *ibid.* **B574**, 675 (2000); V. Barger, S. Geer, R. Raja, and K. Whisnant, Phys. Rev. D **62**, 013004 (2000); M. Freund, M. Lindner, S. T. Petcov, and A. Romanino, Nucl. Phys. **B578**, 27 (2000); A. Cervera, A. Donini, M. B. Gavela, J. J. Gomez Cadenas, P. Hernandez, O. Mena, and S. Rigolin, Nucl. Phys. **B579**, 17 (2000); **B593**, 731 (2001); M. Freund, P. Huber, and M. Lindner, *ibid.* **B585**, 105 (2000); V. Barger, S. Geer, R. Raja, and K. Whisnant, Phys. Lett. B **485**, 379 (2000); Phys. Rev. D **62**, 073002 (2000); **63**, 033002 (2001); **63**, 113011 (2001); M. Campanelli, A. Bueno, and A. Rubbia, Nucl. Phys. **B589**, 577 (2000); A. Bueno *et al.*, hep-ph/0010308; K. Dick, M. Freund, P. Huber, and M. Lindner, Nucl. Phys. **B598**, 543 (2001).
- [19] C. Albright *et al.*, hep-ex/0008064.
- [20] S. M. Bilenky and S. T. Petcov, Rev. Mod. Phys. **59**, 671 (1987).
- [21] S. T. Petcov, Phys. Lett. **110B**, 245 (1982).
- [22] M. Gell-Mann, P. Ramond, and R. Slansky, in *Supergravity*,

- edited by F. Nieuwehuizen and D. Friedman (North-Holland, Amsterdam, 1979), p. 315; T. Yanagida, in *Unified Theories and the Baryon Number of the Universe*, Proceedings of the Workshop, edited by O. Sawada and A. Sugamoto (KEK, Japan, 1979); R. N. Mohapatra and G. Senjanovic, Phys. Rev. Lett. **44**, 912 (1980); see also J. A. Harvey, P. Ramond, and D. B. Reiss, Nucl. Phys. **B199**, 233 (1982).
- [23] S. M. Bilenky, J. Hošek, and S. T. Petcov, Phys. Lett. **94B**, 495 (1980).
- [24] P. Langacker *et al.*, Nucl. Phys. **B282**, 589 (1987).
- [25] B. Kayser and R. Shrock, Phys. Lett. **112B**, 137 (1982).
- [26] Yu. Kobzarev *et al.*, Yad. Fiz. **32**, 1590 (1980) [Sov. J. Nucl. Phys. **32**, 823 (1980)]; M. Doi *et al.*, Phys. Lett. **102B**, 323 (1981).
- [27] M. Moe and P. Vogel, Annu. Rev. Nucl. Part. Sci. **44**, 247 (1994); A. Faessler and F. Šimkovic, J. Phys. G **24**, 2139 (1998).
- [28] H. Ejiri, talk given at “Neutrino 2000” [2].
- [29] L. Baudis *et al.*, Phys. Rev. Lett. **83**, 41 (1999); H. V. Klapdor-Kleingrothaus *et al.* (unpublished); talk given at NOW2000, Otranto, Italy, 2000 (<http://www.ba.infn.it/~now2000>).
- [30] C. E. Aalseth, *et al.*, Yad. Fiz. **63**, 1299 (2000) [Phys. At. Nucl. **63**, 1225 (2000)].
- [31] NEMO3 proposal, LAL Report No. 94-29, 1994; C. Marquet *et al.*, Nucl. Phys. B (Proc. Suppl.) (to be published).
- [32] E. Fiorini, Phys. Rep. **307**, 309 (1998).
- [33] H. V. Klapdor-Kleingrothaus, J. Hellmig, and M. Hirsch, J. Phys. G **24**, 483 (1998); L. Baudis *et al.*, Phys. Rep. **307**, 301 (1998).
- [34] M. Danilov *et al.*, Phys. Lett. B **480**, 12 (2000).
- [35] S. T. Petcov and A. Yu. Smirnov, Phys. Lett. B **322**, 109 (1994).
- [36] S. M. Bilenky, A. Bottino, C. Giunti, and C. W. Kim, Phys. Lett. B **356**, 273 (1995); Phys. Rev. D **54**, 1881 (1996).
- [37] S. M. Bilenky, C. Giunti, C. W. Kim, and S. T. Petcov, Phys. Rev. D **54**, 4432 (1996).
- [38] G. C. Branco, L. Lavoura, and M. N. Rebelo, Phys. Lett. B **180**, 264 (1986).
- [39] J. F. Nieves and P. P. Pal, Phys. Rev. D **36**, 315 (1987).
- [40] P. J. O’Donnell and U. Sarkar, Phys. Rev. D **52**, 1720 (1995).
- [41] J. A. Aguilar-Saavedra and G. C. Branco, Phys. Rev. D **62**, 096009 (2000).
- [42] S. M. Bilenky, C. Giunti, C. W. Kim, and M. Monteno, Phys. Rev. D **57**, 6981 (1998).
- [43] F. Vissani, hep-ph/9708483; J. High Energy Phys. **06**, 022 (1999).
- [44] H. Minakata and O. Yasuda, Phys. Rev. D **56**, 1692 (1997); Nucl. Phys. **B523**, 597 (1998); T. Fukuyama, K. Matsuda, and H. Nishiura, Phys. Rev. D **57**, 5844 (1998); Mod. Phys. Lett. A **13**, 2279 (1998).
- [45] V. Barger and K. Whisnant, Phys. Lett. B **456**, 194 (1999).
- [46] S. M. Bilenky, C. Giunti, W. Grimus, B. Kayser, and S. T. Petcov, Phys. Lett. B **465**, 193 (1999).
- [47] S. T. Petcov, in *Weak Interactions and Neutrinos*, Proceedings of the 17th International Conference, 1999, Cape Town, South Africa, edited by C. A. Dominguez and R. D. Viollier (World Scientific, Singapore, 2000), p. 305.
- [48] S. M. Bilenky and C. Giunti, in *Weak Interactions and Neutrinos* [47], p. 195.
- [49] C. Giunti, Phys. Rev. D **61**, 036002 (2000).
- [50] T. Fukuyama, K. Matsuda, H. Nishiura, and N. Takeda, Phys. Rev. D **62**, 093001 (2000); **63**, 077301 (2001).
- [51] M. Czakon, J. Gluza, and M. Zlarek, hep-ph/0003161Z; M. Czakon, J. Gluza, J. Studnik, and M. Zlarek, hep-ph/0010077.
- [52] H. V. Klapdor-Kleingrothaus, H. Pas, and A. Yu. Smirnov, Phys. Rev. D **63**, 073005 (2001).
- [53] W. Rodejohann, Nucl. Phys. **B597**, 110 (2001).
- [54] S. M. Bilenky, S. Pascoli, and S. T. Petcov, Ref. SISSA 13/2001/EP.
- [55] Super-Kamiokande Collaboration, H. Sobel, talk given at “Neutrino 2000” [2].
- [56] G. L. Fogli, E. Lisi, D. Montanino, and A. Palazzo, Phys. Rev. D **62**, 113003 (2000).
- [57] P. I. Krastev, talk given at NOW2000, Otranto, Italy, 2000 (<http://www.ba.infn.it/~now2000>).
- [58] M. C. Gonzalez-Garcia *et al.*, Phys. Rev. D **63**, 033005 (2001).
- [59] S. T. Petcov, in *Lecture Notes in Physics*, Vol. 512, edited by H. Gausterer and C. B. Lang (Springer, New York, 1998), p. 281.
- [60] S. M. Bilenky, C. Giunti, and W. Grimus, Prog. Part. Nucl. Phys. **43**, 1 (1999).
- [61] B. Pontecorvo, Zh. Éksp. Teor. Fiz. **53**, 1717 (1967) [Sov. Phys. JETP **26**, 984 (1968)]; S. M. Bilenky and B. Pontecorvo, Phys. Rep. **41**, 225 (1978).
- [62] P. I. Krastev and S. T. Petcov, Phys. Lett. B **285**, 85 (1992); **299**, 99 (1993); Phys. Rev. Lett. **72**, 1960 (1994); Phys. Rev. D **53**, 1665 (1996); V. Barger, R. J. N. Phillips, and K. Whisnant, Phys. Rev. Lett. **69**, 3135 (1992); N. Hata and P. Langacker, Phys. Rev. D **56**, 6107 (1997); B. Faïd, G. L. Fogli, E. Lisi, and D. Montanino, Astropart. Phys. **10**, 93 (1999); see also S. L. Glashow and L. M. Krauss, Phys. Lett. B **190**, 199 (1987).
- [63] P. I. Krastev and S. T. Petcov, Phys. Rev. D **53**, 1665 (1996); P. I. Krastev, Q. Y. Liu, and S. T. Petcov, *ibid.* **54**, 7057 (1996).
- [64] M. Appolonio *et al.*, Phys. Lett. B **466**, 415 (1999).
- [65] F. Boehm *et al.*, Phys. Rev. Lett. **84**, 3764 (2000); Phys. Rev. D **62**, 072002 (2000).
- [66] P. Lipari, Phys. Rev. D **61**, 113004 (2000); V. Barger, S. Geer, R. Raja, and K. Whisnant, *ibid.* **62**, 013004 (2000); M. Freund, M. Lindner, S. T. Petcov, and A. Romanino, Nucl. Phys. **B578**, 27 (2000).
- [67] V. Lobashov *et al.*, talk given at “Neutrino 2000” [2].
- [68] C. Weinheimer *et al.*, talk given at “Neutrino 2000” [2].
- [69] A. Aseev *et al.*, talk given at the Intl. Workshop on Neutrino Masses in the sub-eV Range, Bad Liebenzell, Germany.
- [70] E. Gawiser, astro-ph/0005475.
- [71] MAP Collaboration, <http://map.gsfc.gov/>; PLANCK Collaboration, <http://astro.estec.esa.ne/SA-general/Projects/Planck>
- [72] C. Jarskog, Z. Phys. C **29**, 491 (1985); Phys. Rev. D **35**, 1685 (1987).
- [73] P. I. Krastev and S. T. Petcov, Phys. Lett. B **205**, 64 (1988).
- [74] S. M. Bilenky, N. P. Nedelcheva, and S. T. Petcov, Nucl. Phys. **B247**, 589 (1984).
- [75] B. Kayser, Phys. Rev. D **30**, 1023 (1984).
- [76] L. Wolfenstein, Phys. Lett. **107B**, 77 (1981).
- [77] S. T. Petcov, Phys. Lett. **115B**, 401 (1982); **110B**, 245 (1982).
- [78] H. Pas and T. J. Weiler, Phys. Rev. D **63**, 113015 (2001).
- [79] D. Falcone and F. Tramontano, hep-ph/0102136.